



Thermochemical technologies for conversion of biomass and waste into light olefins (C₂-C₄)

Hualun Zhu^a, Mohammed Babkoo^b, Marc-Olivier Coppens^{b,*}, Massimiliano Materazzi^{a,*}

^a Department of Chemical Engineering, University College London, London WC1E 7JE, United Kingdom

^b EPSRC “Frontier Engineering” Centre for Nature Inspired Engineering & Department of Chemical Engineering, University College London, London WC1E 7JE, United Kingdom

ARTICLE INFO

Keywords:

Biomass
Syngas
Gasification
Pyrolysis
Light olefins
Fischer-Tropsch
Catalysis

ABSTRACT

The demand for light olefins, including ethylene, propylene, and butene, continues to grow as they serve as essential intermediates for numerous chemical products. Traditional production methods rely heavily on fossil resources, raising concerns about environmental impact and resource depletion. As the global focus shifts towards sustainability and carbon neutrality, researchers are exploring alternative and renewable feedstocks, such as biomass and waste, to produce light olefins. This review paper provides an in-depth analysis of the recent advancements and strategies employed in the production of light olefins directly and indirectly from biomass and waste via thermochemical processes. Emphasis is placed on the role of catalysis in these approaches, covering catalyst types, applications, and performance. Furthermore, this review explores process intensification approaches as potential avenues for enhancing the efficiency and sustainability of olefin production. By presenting a holistic view of the current state of olefin production from recovered feedstocks, this work aims to contribute to the development of greener and more sustainable bio-based industries, ultimately fostering a transition towards a circular economy and mitigating the environmental impact of the petrochemical industry.

1. Introduction

Light olefins, which include ethylene, propylene and butene, are key intermediates for the production of a wide range of chemical materials and products [1]. Each year, the industry utilizes approximately 1 billion tons of various hydrocarbon feedstocks to produce over 400 million tons of light olefins [2]. In 2022, the global production capacities of ethylene and propylene were estimated to be 225.52 million tons and 150.3 million tons, respectively [3]. Furthermore, the demand for light olefins is projected to grow at a rate of 4–5 % per year [4], with major use in packaging, transportation, electrical and electronic industries, textiles, construction, consumer chemicals, metal industry, coatings, adhesives, food industry, agriculture, medical products, and more [5,6]. Butylene and its C₄ derivatives are essential for producing synthetic rubber, especially for tires and automotive parts. The global market for 1-butylene is expected to reach USD 5.80 billion by 2027, with a growth rate of 3.7 % annually [7].

Traditionally, the production of light olefins relies heavily on the processing of natural gas or crude oil fractions. Approximately 60 % of the global feedstock volume is processed through fluid-catalytic

cracking (FCC) units in oil refineries, while the remaining 40 % is produced in steam cracking (SC) plants [2]. FCC is a conversion process capable of transforming high-molecular weight hydrocarbons, such as crude oils, into gasoline, olefinic gases, and various other products. In the SC process, hydrocarbons predominantly derived from fossil resources are subjected to high temperatures in tubular reactors suspended within a gas-fired furnace. Ethylene is primarily produced through the steam cracking of ethane and naphtha, and modified FCC processes are expected to contribute to increased ethylene production as well. Conventional steam cracking processes boast a thermal efficiency of over 90 % in ethylene production. However, the significant endothermic nature of the process and the intricate cryogenic separation techniques involved make these processes highly energy and carbon intensive. It is estimated that for each ton of ethylene produced, these processes emit 1–2 tons of CO₂, depending on the specific feedstock used [8]. Approximately half of the global propylene production is derived from the steam cracking of naphtha and gas oil, while the other half is generated through conventional FCC units within oil refineries [9]. C₄ hydrocarbons, on the other hand, are predominantly produced as by-products of gasoline production in FCC units. Only a quarter of the

* Corresponding authors.

E-mail addresses: m.coppens@ucl.ac.uk (M.-O. Coppens), massimiliano.materazzi.09@ucl.ac.uk (M. Materazzi).

<https://doi.org/10.1016/j.fuproc.2024.108174>

Received 22 July 2024; Received in revised form 5 December 2024; Accepted 8 December 2024

Available online 24 December 2024

0378-3820/© 2024 The Authors. Published by Elsevier B.V. This is an open access article under the CC BY license (<http://creativecommons.org/licenses/by/4.0/>).

global C₄ hydrocarbon volume originates from the steam cracking of naphtha and gas oil [2]. Four distinct C₄ olefins are of industrial significance: 1-butene, 2-butene, isobutene, and butadiene. When C₄ olefins are present within C₄ fractions, commonly referred to as raffinates, they are typically subjected to further processing [8]. The selection of the most suitable production route is influenced by several factors, including the availability of feedstock, market conditions, price fluctuations, technological maturity, sustainability considerations, and safety aspects [10]. These factors suggest that there may be limited opportunities for further optimization of conventional technologies without substantial process intensification [11].

Due to the finite nature of crude oil and natural gas reserves, their availability will diminish over time, and their extraction will become increasingly expensive [12]. As the demand for light olefins continues to rise, the petrochemical industry is compelled to optimize existing processes to meet capacity demands while simultaneously reducing production costs and environmental impact [5]. Extensive research efforts have been directed towards exploring alternative and economically viable feedstocks for the production of light olefins, taking into account their optimal utilization and high efficiency [1,4,13,14]. Equally important, there is a global imperative to reduce carbon emissions. The emission of CO₂ contributes to global warming, necessitating increased efforts to mitigate emissions and the adverse impacts of climate change [15]. Material efficiency, water conservation, energy efficiency, and greenhouse gas (GHG) emissions are key metrics employed to assess the sustainability of the new processes.

In the quest for sustainable industrial chemical production, biomass and waste have emerged as highly promising alternative feedstocks for the production of light olefins. Second and third-generation biomass, derived from renewable organic waste, offers significant advantages over traditional fossil fuels, including wide availability, relatively low cost, and the ability to be replenished within a short timeframe, unlike finite fossil reserves [13,16,17]. Biomass waste, in the form of agricultural, forestry and other organic residues, represents a significant renewable resource. In the EU, it is estimated that 1466 million tons of agricultural and forestry biomass in dry matter are produced annually, with around 50 % of this are for energy or material use [18]. Globally, the annual generation of biomass waste is around 140 billion tons [19]. This substantial resource base presents significant potential for use in sustainable industrial processes, including the production of bio-based chemicals and fuels.

Notably, a large portion of biomass in many developed countries is found within municipal solid waste (MSW) streams [20]. MSW generation is predicted to grow from 2.1 billion tonnes in 2023 to 3.8 billion tonnes by 2050 [21]. In 2018, Europe produced about 5.2 t of waste per EU inhabitant, with over 60 % being landfilled or incinerated, with detrimental impact on the environment [22]. If the large biogenic fraction of MSW could be recovered or recycled to generate olefins (or previous intermediate products), the contribution towards chemical industry and defossilization of the manufacturing sector would be substantial [20]. The production of light olefins from biomass presents a further advantage by sequestering carbon within the lifetime of the generated chemicals and materials. This process not only reduces emissions from the incineration or decomposition of petroleum-based products but also mitigates carbon emissions throughout the lifecycle of these materials [23].

Additionally, waste streams often contain plastic-based components that cannot be easily recycled with conventional methods, posing a significant environmental challenge due to their potential to contaminate ecosystems and food chains [24]. Diverting non-recyclable waste—approximately 40–50 % of total—from landfills to chemical recycling helps prevent the release of contaminants and microplastics into the environment [25,26]. Thus, by employing biomass and waste in industrial processes, the petrochemical sector can address both carbon feedstock shortages and environmental pollution, while contributing to sustainable waste management and aligning with global sustainability

goals [25,26].

The advancement of greener waste-based industries requires the adoption of a wide array of conversion technologies, encompassing both biochemical and thermochemical processes. Biochemical processes include the utilization of biological mechanisms and microorganisms to transform biomass into biofuels. However, the limitations of biochemical processes include feedstock variability, energy-intensive pretreatment, expensive enzymes, product inhibition, byproduct utilization challenges, competition for feedstock, land and water use concerns [23,27]. These constraints collectively impede their further development and widespread adoption. Thermochemical processes, including gasification, pyrolysis, and hydrothermal liquefaction, are widely regarded as the most promising technologies in the field of waste management and sustainable manufacturing, due to their flexibility and wide range of applications. These technologies do not burn the waste, but instead they decompose it to its fundamental chemical blocks, CO, H₂ or hydrocarbons, from which olefins can be generated via catalytic processing.

Fig. 1 provides a summary of the direct and indirect pathways for converting biomass to light olefins, as discussed in this review. The direct conversion of biomass and waste to light olefins is primarily achieved through pyrolysis. In contrast, indirect conversion processes typically involve a multi-step approach, where biomass is first converted into intermediate products (e.g., syngas or bio-oil) through thermochemical methods, followed by further upgrading or refining to produce light olefins. Recent reviews have comprehensively explored various research aspects within this domain, which include catalyst development [6,28], specific pathways [29,30], products [2,8], feedstocks [4,12,31,32] and catalyst species [33,34]. This review seeks to provide an overview of recent progress in the production of light olefins, directly and indirectly, from biomass and waste feedstocks through thermochemical processes. In particular, this paper examines and evaluates most important pathways for olefin production, taking into account multiple criteria. The study places significant emphasis on the role of catalysis in these approaches, extensively covering topics such as catalyst types, applications, and performance. In addition, importance is placed on the most recent process intensification approaches and their potential advantages in comparison to the state of the art.

2. Biomass to light olefins

The production of light olefins from renewable sources can be carried out starting directly from the bio-feedstock or from certain intermediates (platform molecules) generated by biomass treatment. Biomass-to-olefin processes commence by harnessing feedstocks derived from biomass, encompassing a wide spectrum of organic materials, such as agricultural residues (e.g., crop remnants and straw), forestry waste, dedicated energy crops (e.g., switchgrass), algae, and even MSW. The choice of feedstock carries significant implications for both the economic and ecological dimensions of the process. In addition to biomass, ethanol that is derived from biomass sources like cellulose, corn, and sugarcane, emerges as a preeminent bio-feedstock for olefins production. Furthermore, bio-oil, obtained via catalytic pyrolysis of fats, oils, and other lower-value compounds, also presents a viable feedstock for olefin synthesis. These processes share resemblances with established methodologies within the petrochemical industry.

2.1. Direct conversion (pyrolysis) to light olefins

Pyrolysis is a thermochemical conversion process that involves the decomposition of biomass in the absence of oxygen. It converts the biomass feedstock into hydrocarbons and chemical products, including liquid oil, solid char, and pyrolytic non-condensable gases. Catalytic pyrolysis, in particular, is viewed as a promising technology for the direct conversion of biomass or solid materials into olefins and aromatics within a single reactor [17,30]. The pyrolysis process is classified

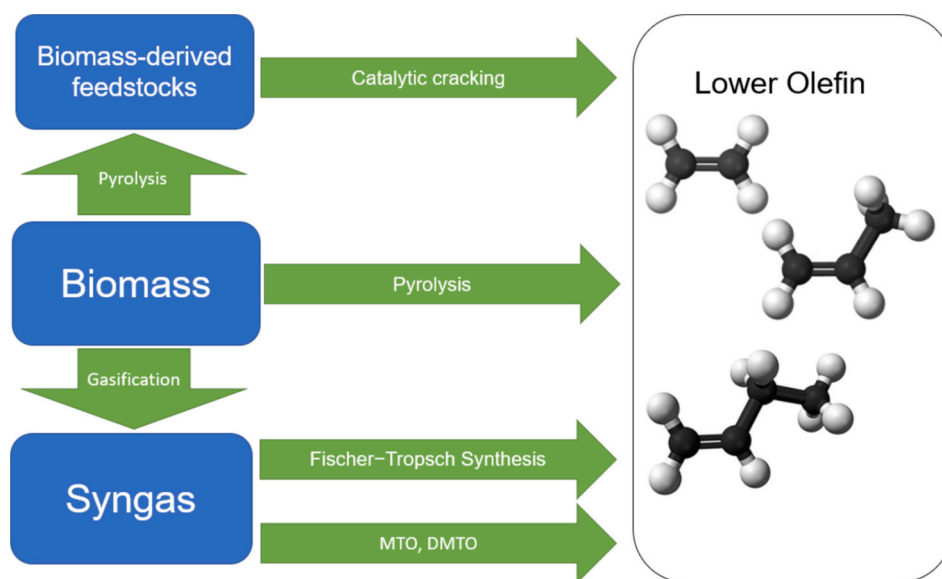


Fig. 1. Direct and indirect conversion of biomass to produce olefins.

into three categories, which are slow, fast, and flash pyrolysis, depending on the operating temperature, heating rate, and reactant residence time [28]. Slow pyrolysis takes place at relatively low temperatures (typically $<300\text{ }^{\circ}\text{C}$) and heating rate ($\sim 10\text{ }^{\circ}\text{C}/\text{min}$) with a residence time longer than 2 s, producing bio-char mostly as the main product. Fast pyrolysis occurs at moderate temperatures ($300\text{--}500\text{ }^{\circ}\text{C}$), short residence time of vapours (less than 2 s), and high heating rate, with products mostly in liquid form. In flash pyrolysis, the feedstock is exposed to high temperatures ($500\text{--}650\text{ }^{\circ}\text{C}$) for less than 1 s, at a very high heating rate. In a comparative study of recycled maize-cob biomass waste, researchers found that fast pyrolysis increased bio-oil yield by 26.5 %, and flash pyrolysis led to a 35.6 % increase in bio-oil yield compared to slow pyrolysis, all conducted at $600\text{ }^{\circ}\text{C}$ under similar conditions [35]. The shorter residence time in fast and flash pyrolysis minimizes secondary reactions that decompose bio-oil into syngas, resulting in higher liquid yields. Thus, the choice of pyrolysis type significantly impacts product distribution.

The common types of reactors used in pyrolysis include fixed bed, fluidized bed, circulating fluidized bed, ablative, rotating cone, auger, vacuum, solar and microwave [36]. Fixed bed reactors appear to be still the most popular reactor type, especially at small scale, adopted in $\sim 70\%$ of the most recent and most cited research papers reviewed in this work. Fluidized bed reactors come after, more favoured in medium-large scale applications [28]. The operating parameters of pyrolysis have strong influences on the yield and the composition of products including feedstock, particle size, catalyst, operating temperature, heating rate, residence time, and type of carrier gas [32,37–39]. The catalytic pyrolysis process shows a high energy conversion efficiency, and pyrolysis of waste, especially waste plastics, has gained more attention in recent years, since it achieves environmentally friendly conversion of plastic solid waste into highly valuable fuels and chemicals [17]. However, for catalytic pyrolysis of biomass and plastic, relatively low yields of light olefins were usually reported based on in-situ catalysis. Light olefins are mostly considered as secondary products, although liquid product (oils) can be further cracked to produce light olefins.

Biomass is oxygen-rich and composed of lignin, cellulose, and hemicellulose, requiring catalysts like ZSM-5 to deoxygenate and break down larger molecules. However, biomass pyrolysis produces oxygenated byproducts such as CO, CO_2 , and water, resulting in lower light olefin yields and catalyst deactivation due to coking [40]. On the other hand, plastic waste, composed of long hydrocarbon chains, lacks oxygen, making pyrolysis more efficient for producing $\text{C}_2\text{--}\text{C}_4$ olefins.

Catalysts used in plastic pyrolysis focus on cracking polymers, leading to higher selectivity for light olefins without oxygen-related byproducts [41]. While biomass pyrolysis faces difficulties with catalyst stability and lower olefin yields, plastic waste pyrolysis offers a more efficient route to olefins but raises environmental concerns related to waste and emissions [42].

Fig. 2 illustrates the potential routes and resulting products obtained from both non-catalytic and catalytic pyrolysis processes applied to cellulose, as reported by Huang et al. [43]. ZSM-5 is one of the most commonly used catalysts for biomass pyrolysis [44]. In the initial stages of pyrolysis, larger biomass-derived molecules are thermally degraded into smaller fragments, including oxygenates, aromatics, and light hydrocarbons [45]. ZSM-5 facilitates the further cracking of these fragments, particularly oxygenates, by providing strong acid sites where protonation and deoxygenation can occur [46]. In addition to ZSM-5, other catalytic systems, such as SAPO-34 and MCM-41, have been explored for their ability to promote olefin production during pyrolysis. SAPO-34, with its smaller pore structure, exhibits excellent selectivity towards light olefins, while MCM-41, a mesoporous material, offers enhanced diffusion properties [47,48].

Funazukuri et al. [49] studied cellulose flash pyrolysis to produce olefins at $275\text{--}720\text{ }^{\circ}\text{C}$ for 0.5–20 s using a pyroprobe reactor. They found that the lighter olefins yield could reach 9 wt%, and ethylene accounted for more than 50 % of the produced olefins by weight [49]. More recently, Carlson et al. produced olefins using ZSM-5 catalyst with three different reactors, including a semi-batch reactor, a fixed bed reactor and a fluidized bed reactor; they used model compounds and biomass as feedstocks [50]. Olefins were obtained from pine sawdust with the highest yield of 9.2 mol% in the fluidized bed reactor at biomass weight hourly space velocities (WHSV) of 0.8 h^{-1} and $670\text{ }^{\circ}\text{C}$, with aromatics yield of 9.3 mol%. They also concluded that ethylene selectivity remained quite stable at 41.0–45.7 %, while propylene selectivity sharply decreased from 22.1 % to 0.8 % when pyrolysis temperature increased from $500\text{ to }670\text{ }^{\circ}\text{C}$ [50]. Yields of light olefins decreased with WHSV and increased with temperature in the fixed bed reactor. The highest olefins yield of 19.4 mol% was obtained at $\text{WHSV} = 10.4\text{ h}^{-1}$ and pyrolysis temperature of $650\text{ }^{\circ}\text{C}$ over ZSM-5, with 20.9 mol% aromatics yield. The semi-batch reactor yielded the highest amount of aromatics, while the combined yield of aromatic and olefin products was higher in the fixed and fluidized bed reactors [50].

Zhang et al. [17] found that LOSA-1, which is primarily composed of ZSM-5, was effective in producing olefins and aromatics. They achieved

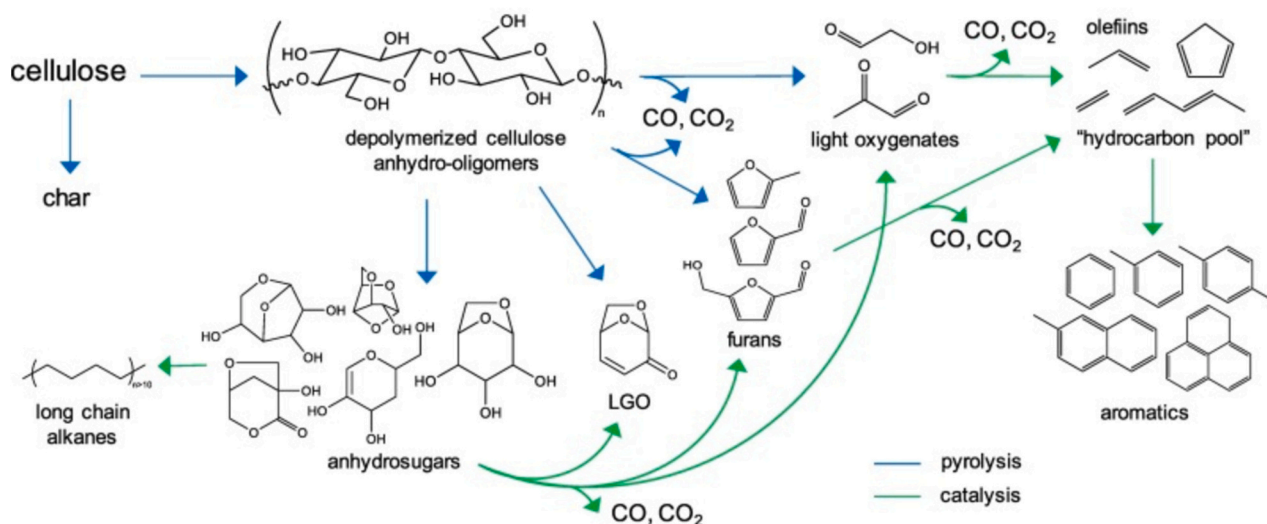


Fig. 2. Pyrolysis of cellulose to value-added chemicals [43].

a maximum yield of 8.5 %C for olefins through the in situ continuous pyrolysis of rice stalk in a fluidized bed reactor at 550 °C. When LOSA-1 was mixed with meso- and macroporous $g\text{-Al}_2\text{O}_3$, CaO, and MCM-41, the olefins yield increased to some extent, with the highest yield of 11.2 mol % observed over 10 % $\text{Al}_2\text{O}_3/\text{LOSA-1}$. They concluded that the meso- and microporous catalysts broke down larger oxygenates into smaller ones, while LOSA-1 promoted the formation of olefins and aromatics from the smaller oxygenates. The researchers also studied the production of olefins using proprietary ZSM-5 (composed of ZSM-5, $\gamma\text{-Al}_2\text{O}_3$) and spent FCC catalysts, which yielded 10.5 and 5.7 mol% of olefins, respectively [51].

Using steam to pretreat ZSM-5 was found to be effective in adjusting its porous properties and acid sites through framework dealumination. After steam treatment, the number of micropores in ZSM-5 decreased while mesopores increased, allowing for more primary cellulose volatiles to diffuse. At the same time, the number of weak acid sites increased while the number of strong acid sites decreased, which prevented further reactions of olefins to form aromatics within the pore network of ZSM-5. This led to an increase in olefins yield. The maximum yield of olefins obtained for the pyrolysis of cellulose was 17 mol% over steam pretreated ZSM-5 under 60 % steam atmosphere [52].

Pretreated, modified and metal-loaded ZSM-5 is considered effective to increase olefins yield in direct pyrolysis of biomass. Huang et al. [53] investigated the influence of loading La onto ZSM-5 through in situ pyrolysis of cellulose in a fixed reactor. They found that increasing the number of medium acid sites by modifying ZSM-5 with La was favorable for olefin formation. The results showed that the optimized yield of olefins was 30.9 mol% at 600 °C with a gas residence time of 10 s at a catalyst to feed ratio of 2. The use of other feedstocks such as lignin, sawdust, rice husk, and hemicellulose produced olefins with yields of 8.6, 14.7, 20.1, 21.2, and 27.6 mol%, respectively [53].

Researchers investigated the influence of various parameters on olefin production, including the type of pyrolysis, pyrolysis temperature, catalyst to feed ratio, gas flow rate, and types of active metals used [54–56]. The results indicated that ex situ pyrolysis resulted in a higher olefins yield compared to in situ pyrolysis, and that increasing the gas flow rate did not have a significant effect. Increasing the pyrolysis temperature had an initially positive impact on olefins yield until 600 °C. The use of ZSM-5 loaded with different metals had a notable impact on the distribution of olefins yield, where Ce-, Mg-, and P-modified ZSM-5 catalysts could promote olefin formation, but Fe-modified ZSM-5 had little effect. Ce-modified ZSM-5 produced the highest yield of olefins at 9.2 mol%, followed by Mg-, P-, and Fe-modified ZSM-5 catalysts.

Researchers have conducted investigations into the co-pyrolysis of

pine and low-density polyethylene (LDPE) with the aim of enhancing the production of light olefins and aromatics. Various catalysts, including calcium oxide, calcium aluminate, calcium ferrite, ZSM-5, and FCC, were employed in these studies [57]. The results demonstrated a positive synergistic effect in the co-pyrolysis of pine and LDPE, and the incorporation of a catalyst was found to substantially reduce the average apparent activation energy of the co-pyrolysis process. Among the catalysts tested, calcium aluminate (CaAl) and ZSM-5 with Si/Al ratios of 40 (Z40) emerged as the most optimal base and acid catalysts, respectively. The highest yield of light olefins (~25 %) was achieved when utilizing a base-acid tandem catalyst (CaAl-Z40) at 600 °C, with a CaAl to Z40 ratio of 1:1.

Table 1 presents the production yields of light olefins obtained directly from the catalytic pyrolysis of biomass using different catalysts reported in the literature. Among these catalysts, modified ZSM-5 with increased mesopores shows considerable promise for enhancing olefin production. Nevertheless, the persistent challenge of coke deposition necessitates substantial research efforts in the design and development of catalysts with enhanced tolerance to coke formation. Addressing this issue is vital for further advancing the efficiency and feasibility of the catalytic pyrolysis process. The incorporation of an additional catalytic stage for the conversion of naphtha by-products from pyrolysis into olefins offers numerous advantages, including the potential to elevate olefin yields, refine process selectivity, and mitigate by-product generation [6,58]. This supplemental catalytic step is poised to augment the overall efficacy of biomass utilization. The next section will delve into the merits and technical intricacies associated with this ancillary catalytic conversion.

2.2. Conversion of biomass-derived feedstocks into light olefins

Utilizing liquid oil generated from biomass pyrolysis to produce light olefins offers a sustainable and potentially viable alternative to the traditional reliance on naphtha and petroleum sources [17,30,64]. The catalytic cracking technology extensively employed in the oil refinery industry shares similarities with that for the conversion of biomass-derived feedstocks into valuable products. However, to optimize the process, it is crucial to enhance the selectivity of light olefins. The yield of light olefins from bio-oil is generally lower compared to traditional petrochemical processes like naphtha steam cracking, a well-established process that typically achieves ethylene yields of around 30–35 % and propylene yields of 15–20 % [65,66]. In contrast, bio-oil, produced from biomass via pyrolysis or other methods, contains a mixture of oxygenated compounds, making direct conversion into olefins more

Table 1
Catalytic pyrolysis of biomass and waste to light olefin production.

Feedstock	Reactor	Condition	Catalyst	Product yield (C-mol%)	Remarks	Year and reference
Pine sawdust	Continuous pyrolysis in a fluidized bed reactor	670 °C, 1 bar, 1200 sccm He fluidization flow rate, WHSV: 0.8 h ⁻¹	ZSM-5	9.3 % aromatics, 9.2 % olefins, 10.9 % CH ₄ , 30 % CO, 9.1 % CO ₂ , 23.8 % coke.	> 95 % ethylene selectivity in produced olefins	2011 [50]
Rice stalk (3.0 wt% moisture, 66.3 wt% volatile, 16.3 wt% fixed carbon and 14.5 wt% ash)	Continuous pyrolysis in a fluidized bed reactor	550 °C, 1 bar, 0.5 L/min N ₂ , 44 g/h rice stalk.	Al ₂ O ₃ /LOSA-1 (Al ₂ O ₃ 10 %)	14.1 % aromatics, 11.2 % olefins, 24.8 % CO, 14.0 % CO ₂ , 24.8 % coke.	Olefin selectivity: ethylene: 59.1 %, propylene: 39.9 %, butene: 1.1 %	2013 [17]
Rice stalk (3.0 wt% moisture, 66.3 wt% volatile, 16.3 wt% fixed carbon and 14.5 wt% ash)	Continuous pyrolysis in a fluidized bed reactor	550 °C, 1 bar, 0.5 L/min N ₂ , 44 g/h rice stalk.	LOSA-1, CaO/LOSA-1, MCM-41/LOSA-1, ZSM-5	ZSM-5: 12.8 % aromatics, 10.5 % olefins, 20.7 % CO, 12.8 % CO ₂ , 32.2 % coke. LOSA-1, CaO/LOSA-1, MCM-41/LOSA-1 achieved olefins yield of 8.5, 9.6, 9.8, 10.5 mol%, respectively.	ZSM-5 Olefin selectivity: ethylene: 51.5 %, propylene: 47.4 %, butene: 1.1 %	2013 [51]
Pine sawdust	Continuous pyrolysis in a two-stage (pyrolysis-catalysis) reactor	550 °C, 1 bar, N ₂ to steam ratio varied from 0 to 60 %, WHSV 1.33 h ⁻¹	ZSM-5	17 % olefins, 7 % aromatics, 3 % CH ₄ , 18 % CO, 8 % CO ₂ , 25 % coke and char.	An increased steam concentration resulted in higher olefin yields, higher propylene selectivity and lower ethylene selectivity.	2020 [52]
Cellulose	In situ catalytic pyrolysis in a fixed bed reactor	600 °C, 1 bar, catalyst/feed = 3, residence time: 10 s	La/ZSM-5 (6 wt%)	30.9 % olefins, 18.3 % CO, 10.1 % CO ₂ , 7.4 % CH ₄ , 29.0 % coke.	ethylene: 54.0 %, propylene: 40.9 %, butene: 5.1 %	2012 [53]
Hemicelluloses, cellulose, lignin, and corn stalk	Ex situ pyrolysis in a fixed bed reactor	600 °C, 1 bar, catalyst/feed = 2	Fe/ZSM-5 (3 wt%)	Cellulose showed the highest olefin yield: 6.98 %, with 13.29 % CO, 5.04 % CO ₂ , 1.23 % CH ₄ , and 35.77 wt% coke, 34.99 wt% oil. Lignin, hemicellulose, and corn stalks led to olefins yields of 1.39 %, 4.50 %, and 5.27 %, respectively.	Cellulose olefins selectivity: ethylene: 79.00 %, propylene: 19.50 %, butene: 1.50 %	2018 [59]
Wheat straw	Ex situ pyrolysis in a fixed bed reactor	600 °C, 1 bar, catalyst/feed = 8	Ce, Mg, Fe, P/HZSM-5 (5 %)	Ce-, Mg-, Fe-, and P/HZSM-5 resulted in olefins yield of 9.2, 8.3, 7.0, and 7.7 %-C, respectively.	Ce/ZSM-5 olefin selectivity: ethylene: ~57 %, propylene: ~40 %, butene: ~3 %	2019 [56]
Pine wood	Ex situ pyrolysis in a fixed bed reactor.	500 °C, 1 bar, catalyst/feed = 1	Sn/M-ZSM-5	12.5 % olefins, 20.0 % aromatics, 2.0 % CH ₄ , 8.5 % CO, 3.5 % CO ₂ , 28 wt% oil.	The hollow structure and the reduced strong acidic sites of Sn/M-ZSM-5 limited the alkylation and aromatization reactions of olefins.	2021 [60]
HDPE	Pyrolysis in a batch reactor	380 °C, 1 bar, catalyst/feed = 0.01	Conventional, hierarchical Beta,	~13 % aromatics, ~30 % alkanes, ~25 % olefins,		2017 [61]
Pine sawdust and LDPE (1:1)	Pyrolysis in TG-FTIR reactor	600 °C, 1 bar, catalyst/feed = 4	ZSM-5 with different Si/Al ratios (40, 80, 200)	ZSM-5(200) showed highest olefins yield (33.4 %), with ~15 % MAH, 30 % BTX, 12 % PAH, and ~20 % other hydrocarbons.	Selectivity to butenes in olefins >60 %, co-pyrolysis of pine and LDPE showed a positive synergistic effect.	2023 [57]
LDPE	Microwave pyrolysis in a tubular reactor	375 °C, 1 bar, catalyst/feed = 0.1	Al-SBA-15, Al-MCM-41, xWZr, P-SiO ₂ , Zeolite HY (30)	Al-SBA-15 showed the highest conversion (>90 %), highest C ₂ -C ₄ olefin yield (~24 %), with ~55 % C ₅₊ olefins and ~12 % alkanes.	The olefin selectivity follows Al-SBA-15 > Al-MCM-41 > xWZr > P-SiO ₂ > HY(30).	2023 [62]
Wheat straw and HDPE (3:1)	Pyrolysis in a two-stage fixed-bed reactor	500 °C, 1 bar, catalyst/feed = 0.1	Mn, Ni, Zn/ZSM-5	5 % Mn-HZSM-5: 30 wt% gas yield (selectivity: ~30 % alkanes, ~16 % olefins, ~27 % CO, ~28 % CO ₂), 42 wt% liquid yield and 28 wt% solid yield.	5 % Mn-ZSM-5 light olefins selectivity in gas product at 15.84 % followed by 1 % Mn (13.97 %) and 10 % Ni (13.61 %) respectively.	2023 [63]

challenging. This section provides an overview of previous research endeavours that have specifically focused on improving olefin selectivity in the catalytic cracking of biomass pyrolysis vapours and bio-oil.

The selectivity of bio-oil conversion to light olefins can be influenced by modifying experimental conditions, such as reaction temperature and residence time. In their study, Gayubo et al. [67] employed a thermal-catalytic conversion system, using HZSM-5 zeolite (SiO₂/Al₂O₃ = 80) as a hydrothermally stable catalyst. The researchers investigated various operating conditions, including the methanol content added to raw bio-oil, temperature, and space-time. Notably, they achieved a bio-oil

conversion rate of 94 % with an impressive olefins selectivity of 48 wt% by employing a bio-oil/methanol feed ratio of 50/50 wt% at 500 °C and a space-time of 0.37 kg_{catalyst}h/(kg_{feed})⁻¹. These findings provide a valuable foundation for further research on co-processing raw bio-oil with methanol in the methanol-to-olefins (MTO) process.

Vispute et al. [68] employed a comprehensive method that combines hydroprocessing of bio-oil using supported metal catalysts, followed by cracking utilizing zeolite-based catalysts. The initial hydrogenation using Ru/C and Pt/C catalysts led to the stabilization of bio-oil, while increasing its intrinsic hydrogen content, resulting in the production of

polyols and alcohols. Subsequently, upgrading the hydrogenated bio-oil over HZSM-5 zeolite facilitated the conversion into light olefins and aromatics, achieving a yield up to three times higher than that obtained from untreated bio-oil. The findings from the study also demonstrated that increasing the H/C_{eff} ratio of the feed contributes to the enhancement of olefins production. Moreover, it was observed that the catalyst deactivation caused by coke deposition decreases significantly under such conditions.

Gong et al. [69] conducted a study on the selective production of light olefins through catalytic cracking of raw bio-oil using La-modified HZSM-5 catalyst. By incorporating La into the zeolite structure, they observed a moderate increase in medium acid sites, which effectively improved the selectivity to light olefins and enhanced the catalyst's stability. The study resulted in the highest light olefins yield of $0.28 \text{ kg}_{\text{olefins}}(\text{kg}_{\text{bio-oil}})^{-1}$, with almost complete conversion of the bio-oil. The authors later achieved similar results when using Mg to modify the acidity of HZSM-5 zeolite. The addition of Mg to the catalyst also enhanced olefins selectivity and catalyst stability, leading to an olefins yield of $0.25 \text{ kg}_{\text{olefins}}(\text{kg}_{\text{bio-oil}})^{-1}$ and nearly complete bio-oil conversion [70]. Furthermore, the same research group investigated the production of olefins by directly mixing the catalyst (La–HZSM-5) with dry biomass, specifically sugarcane. This approach resulted in a yield of $0.12 \text{ kg}_{\text{olefins}}(\text{kg}_{\text{bio-oil}})^{-1}$ [71].

The effective conversion of bio-oil might require a multi-step catalytic process depending on the final product of interest, which can see light olefins only as intermediates. For example, the catalysts can involve both metal and acid sites to produce olefins, followed by the cyclization of these olefins on acid sites to form cycloalkanes, and finally, the dehydrogenation of cycloalkanes on metal sites to yield aromatics. The judicious selection of appropriate metal catalysts has proven to be efficient in controlling the selectivity of these reactions. Zhang et al. [60] conducted an integrated catalytic transformation study, wherein they employed a La/HZSM-5 catalyst to catalytically crack bio-oil into light olefins and subsequently utilized metal oxides-modified ZSM-5 zeolite to oligomerize these to higher molecular

weight products. Under carefully optimized reaction conditions, the process achieved a maximum yield of $0.19 \text{ kg}/(\text{kg}_{\text{bio-oil}})$ of gasoline-range biofuel with significantly reduced oxygen content, high research octane number (RON), and high low heating value (LHV). Table 2 summarizes literature data on the catalytic conversion of biomass-derived feedstocks into light olefins.

3. Syngas to olefins

The other important technology in thermochemical biorefinery concepts is gasification. Differently from pyrolysis, gasification promotes the production of gaseous product (syngas), which can be used as reactive mixture for chemicals (including olefins) synthesis. Gasification of biomass offers several advantages compared to pyrolysis, including higher flexibility on feedstock acceptance and greater control on product distribution. Syngas, generated by the gasification of solid feedstock in presence of limited amount of oxygen, is a gaseous mixture composed of hydrogen (H_2) and carbon monoxide (CO) mostly, with varying quantities of Carbon dioxide (CO_2), methane (CH_4) and light hydrocarbons. Once cleaned from tars and inorganic contaminants, syngas can be used as gaseous feedstock to synthesise a wide range of chemical products, including chemicals (hydrogen, methanol) and hydrocarbons (methane, light olefins, kerosene, etc.), through well-established chemical processes developed over the last decades in the chemical industry [33,73,74]. While syngas is traditionally produced from coal, natural gas, residual oils, and petroleum, the syngas derived from biomass and waste is considered a more sustainable alternative and has garnered significant research attention [75,76]. Biomass has been reported to produce syngas with a higher H_2/CO ratio compared to coal and natural gas, though it exhibits a lower heating value per kilogram of feedstock. However, integrating the water-gas shift reactions within the same apparatus to adjust the H_2/CO ratio provides significant flexibility in controlling the composition of the feed gas [77,78]. The most common sources for bio-syngas production are lignocellulosic materials derived from agricultural and agroforestry activities, such as sugarcane

Table 2
Catalytic conversion of biomass and waste derived feedstocks into light olefins.

Feedstock	Reactor	Condition	Catalyst	Product yield	Remarks	Year and reference
Pine bio-oil + MeOH (50/50 wt%)	Continuous cracking in a fluidized bed reactor	500 °C, 1 bar, catalyst/feed = 0.37	ZSM-5 (80)	41 wt% C ₂ -C ₄ olefins, 6 wt% C ₂ -C ₄ paraffins, 21 wt% aromatics, 30 wt% C ₅₊	Olefin selectivity: 20 % ethylene, 56 % propylene, 24 % butene.	2010 [67]
Pine bio-oil	Continuous cracking in a fluidized bed reactor	450 °C, 1 bar, catalyst/feed = 0.37	ZSM-5 (80)	24 wt% C ₂ -C ₄ olefins, 2 wt% C ₂ -C ₄ paraffins, 50 wt% aromatics, 12 wt% C ₅₊	Olefin selectivity: 26 % ethylene, 58 % propylene, 16 % butene.	2010 [67]
Pinewood bio-oil	Continuous cracking in a fluidized bed reactor	600 °C, 1 bar, WHSV 3 h ⁻¹	HZSM-5 (30)	11.2 % C ₂ -C ₄ olefins, 18.3 % CO and CO ₂ , 9.8 % aromatics, 49.8 % coke.	Olefin selectivity: 51.8 % ethylene, 36.6 % propylene, 11.6 % butene.	2010 [68]
White oak bio-oil	Continuous cracking in a fixed-bed reactor	600 °C, 1 bar, WHSV 11.7 h ⁻¹	HZSM-5 (30)	12.5 % C ₂ -C ₄ olefins, 11.5 % aromatics, 5 % CO ₂ , 17 % CO, 19 wt% coke.	Olefin selectivity: 52 % ethylene, 37 % propylene, 11 % butene.	2011 [64]
Straw stalk bio-oil	Continuous steam cracking in a fixed-bed reactor	600 °C, 1 bar, S/C = 5.0, WHSV 0.4 h ⁻¹	La(6 %)/ZSM-5	95 % carbon conversion, 28 wt% olefin yield. Gas selectivity: 58 % C ₂ -C ₄ olefins, 7 % CH ₄ , 19 % CO ₂ , 18 % CO, 7 % C ₅₊	Olefin selectivity: 34 % ethylene, 56 % propylene, 10 % butene.	2011 [69]
Straw stalk bio-oil	Continuous steam cracking in a fixed-bed reactor	600 °C, 1 bar, S/C = 4.6, WHSV 0.4 h ⁻¹	Mg (5 %)/ZSM-5 (25)	93 % carbon conversion, 25 wt% olefin yield. Gas selectivity: 59.8 % C ₂ -C ₄ olefins, 8.1 % CH ₄ , 18.2 % CO ₂ , 3.2 % CO, 7 % C ₅₊	Olefin selectivity: 39 % ethylene, 50 % propylene, 11 % butene.	2013 [70]
Marine plastic litter (ML) naphtha, MPW naphtha	Continuous steam cracking in a fixed-bed reactor	880 °C, 1.7 bar, steam:feed(wt) = 0.5, residence time 0.48–0.57 s	–	ML naphtha: 31.3 % C ₂ -C ₄ olefins, 24.8 % aromatics, 12 % CH ₄ , 1.2 % CO. MPW naphtha: 43.1 % C ₂ -C ₄ olefins, 17.9 % aromatics, 14 % CH ₄ , 0.9 % CO.	ML naphtha Olefin selectivity: 57 % ethylene, 26 % propylene, 17 % butene. MPW naphtha: 63 % ethylene, 24 % propylene, 13 % butene	2022 [72]

bagasse, rice straw, corn straw, and soybean straw, because they lead to relatively high conversion into H_2 and CO [75,79–81]. However, it is the syngas production from biomass waste and non-recyclable plastics that has attracted renewed interest in the past 20 years [82]. Nevertheless, less refined feedstock introduces new levels of complexities, with relation to gas cleaning and plant availability. Contaminants are commonly found in waste-derived syngas including particulate matter, tars, sulfur compounds, nitrogen compounds, alkali metals, chlorine and heavy metals [75]. Therefore, syngas requires extensive purification processes before being used in catalytic processes for chemical synthesis.

Once cleaned, there are two main approaches for converting syngas into light olefins: indirect and direct processes. In the indirect process, syngas is first converted into an intermediate product, such as methanol, Fischer-Tropsch liquids, or dimethyl ether (DME), which can then be further transformed into light olefins using processes like MTO, dehydration, cracking, or dimethyl ether to olefins (DMTO). On the other hand, by combining some of these processes into one, syngas can be directly converted into light olefins, thus reducing plant costs, and improving efficiencies. Fig. 3 provides a summary of the conversion processes involved in the production of light olefins from syngas, encompassing both direct and indirect pathways.

3.1. Direct Processes of light olefins from syngas

In the direct process, syngas is directly converted into light olefins through either Fischer-Tropsch synthesis (FTS) or the Oxide-Zeolite (OX-ZEO) process. The direct conversion of syngas into light olefins via Fischer-Tropsch to olefins (FTO) has been studied for over 50 years and has recently gained increasing interest. The process has its origin in the first hydrocarbon synthesis reaction, which was reported in 1902 [83]. FTS is a process that converts CO and H_2 into hydrocarbons and alcohols in the presence of a catalyst. The FTO process aims to optimize the production of light olefins, minimize methane yield, and prevent additional CO_2 formation. However, commercial or industrial applications of FTO are rarely reported due to low C_2 - C_4 olefin selectivity and low mechanical or chemical catalyst stability [6]. The product distribution in the FTO process can be predicted using the Anderson-Schulz-Flory (ASF) model. Process conditions, type of catalyst, and promoters can influence the chain growth probability and further impact the product

distribution. Despite tremendous efforts, low selectivity towards light olefins remains a major issue in FTS. This issue arises due to the inherent polymerization nature of the FTO reaction, wherein CH_2 monomers incrementally append to the growing chain until termination takes place [84]. According to the ASF model, the highest selectivity to C_2 - C_4 hydrocarbons (including both olefins and paraffins) is around 57 % [14]. Researchers have focused on catalyst and promoter development to produce more C_2 - C_4 olefins, less methane, and CO_2 . The choice of catalysts in FTO is based on factors such as catalytic activity and stability, selectivity to light olefins, and bond strength [85]. Bond strength, determined by the electronic properties of the atoms involved in the reaction, heavily impacts the number of reactions occurring during the FTS process. Catalyst basicity, dispersion, active metals, promoters, and interaction with the support material significantly influence the FTS process's selectivity towards light olefins [10,85,86]. The first FTS plant using natural gas was pioneered by Shell in Bintulu, Malaysia, in 1993. These facilities employed cobalt-based catalysts (Co/SiO_2 , Co/TiO_2) within a multitubular fixed-bed reactor, and they utilized a low-temperature Fischer-Tropsch (LTFT) technology [87]. Today, FTS finds industrial application in only a limited number of countries. Notably, South Africa hosts four operational FTS plants managed by Sasol. In Qatar, two FTS facilities are presently operational: Oryx GTL, a collaborative venture involving Qatar Petroleum and Sasol, and Pearl GTL, a joint effort between Qatar Petroleum and Shell. Of particular significance, Pearl GTL holds the distinction of being the largest FTS plant globally, boasting an impressive daily production capacity of 140,000 barrels. It is worth noting, however, that the total investment cost incurred for Pearl GTL significantly exceeded the initial estimates, reaching a substantial figure of \$18 billion USD [1]. It is also reported that medium-temperature Fischer-Tropsch synthesis technology, developed by Synfuels China, outperformed conventional low-temperature slurry-bed processes by utilizing only about one-fourth of the solid catalyst charge due to an ultra-active F-T synthesis catalyst, efficiently converting FTS reaction heat into steam up to 30 bar, producing high-quality FTS syncrudes with significantly reduced oxygenates, particularly acids, and offering easy retrofit capabilities the processes [88,89]. Since 2009, Synfuels China has successfully commissioned and operated two demonstration plants, each with a capacity of 160,000 tons per year, employing the high-temperature ($275\text{ }^\circ\text{C}$) slurry phase Fischer-Tropsch

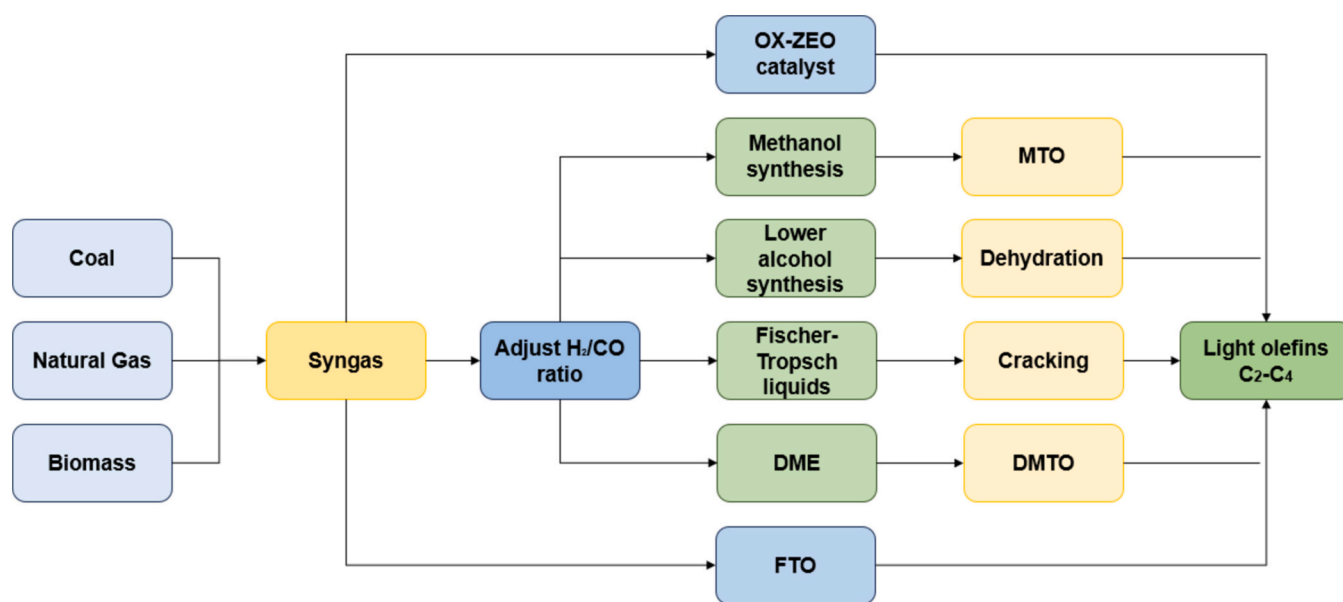


Fig. 3. Processes for the transformation of syngas into light olefins. The light-green and light-yellow boxes represent the indirect pathways, while the blue boxes indicate the direct pathways from syngas to light olefins. (For interpretation of the references to colour in this figure legend, the reader is referred to the web version of this article).

process technology [89]. The experience gained from these projects, particularly in the realm of process engineering, has facilitated the company's scale-up to a commercial-scale plant with a capacity of 4 million tons per year, commissioned in January 2017 [89].

The development of catalysts considers three crucial factors: activity, selectivity, and stability, all of which strongly influence the feasibility of industrial-scale application via FTO. Fe and Co are the most common metals used in FTO catalysts. At lower temperatures, Fe catalysts demonstrate heightened selectivity towards paraffins, while a temperature increase prompts a shift in selectivity towards olefins [5,85]. The process of FTS leads to the formation of iron carbides owing to the analogous activation energy involved in both CO hydrogenation and iron carbide generation [80,85,90]. Different forms of iron carbides have been determined during FTS, and promoters can also affect FTO catalysts and their selectivity.

The most common compounds in iron-based catalysts include iron carbide, metallic Fe and magnetite (Fe_3O_4) [10,91]. Iron carbide is usually in the form of $\epsilon\text{-Fe}_2\text{C}$, $\epsilon'\text{-Fe}_{2.2}\text{C}$, Hägg $\gamma\text{-Fe}_5\text{C}_2$, Fe_7C_3 , or $\theta\text{-Fe}_3\text{C}$ [85]. $\gamma\text{-Fe}_5\text{C}_2$ is considered as most active phase under typical FTS temperature (240–360 °C) [92]. Jiang et al. [93] performed a series of experiments on iron-based catalysts to investigate the catalytic activity, selectivity and deactivation in FTS process using $\gamma\text{-Al}_2\text{O}_3$, SiO_2 , activated carbon (AC), anatase- TiO_2 and SiC as support with different promoters (K, Na, and S). They concluded that the catalytic activity depends on the iron oxide reducibility, which is further influenced by the particle size-dependent carburization, promoter effects, interaction of metal (Fe) with the support, and the particle size. The $\text{C}_2\text{-C}_4$ olefin selectivity can also exceed the limitation of the ASF distribution using K, Na, and S. Finally, the reversible transformation of $\gamma\text{-Fe}_5\text{C}_2$ into Fe_3O_4 and K-induced carbon deposition were highlighted as reasons for catalyst deactivation [93]. Fig. 4 illustrates the carburization behaviour of various reduced iron phases in the context of an iron-based catalyst. Similar studies have been carried out to determine the precise atomic arrangement of the $\epsilon\text{-Fe}_2\text{C}$ and $\epsilon'\text{-Fe}_{2.2}\text{C}$ phases in iron-based FTS catalysts. They noted that the unit cell of $\epsilon\text{-Fe}_2\text{C}$ has only one chemical

environment for Fe atoms, whereas $\epsilon'\text{-Fe}_{2.2}\text{C}$ features six distinct chemical environments for Fe atoms [94].

Cobalt-based catalysts usually show high catalytic activity, low WGS activity, and superior stability. Therefore, they always require higher H_2 to CO ratio (2.0–2.2) compared to Fe [85,95]. To enhance the selectivity of cobalt-based catalysts towards light olefins for industrial use, noble metals, transition metal oxides, and alkali metal oxides are recommended as promoters, since Co is not selective to light olefins for industrial application [85].

Fig. 5 provides a comprehensive representation of the reaction mechanism and catalytic performance for the FTO process. Fig. 5A illustrates a schematic diagram of the mechanistic model, highlighting the role of direct olefin re-adsorption and the involvement of two distinct surface intermediates. This schematic provides insights into the pathways influencing olefin production, the desorption of $\text{C}_{n\alpha, \text{ads}}$ and $\text{C}_{n\beta, \text{ads}}$ ($n = 2, 3$) is the key point for increasing ethylene and propene selectivity. Fig. 5B presents the selectivity of light olefins for various cobalt-based FTO catalysts across different temperature conditions [97]. The atomic ratio of cobalt to other metals was consistently maintained at 2. Catalysts, including CoMn, CoCe, CoLa, and CoAl composite oxides, were synthesized via the co-precipitation method, while the Mn/Co sample was prepared through the impregnation method. Except for the Mn/Co catalyst, all metal oxide promoters improved $\text{C}_2\text{-C}_4$ olefins selectivity, and the $\text{C}_2\text{-C}_4$ olefins selectivity of the catalysts followed the trend $\text{CoMn} > \text{CoCe} > \text{CoLa} > \text{Co}_3\text{O}_4$, with selectivity decreasing as reaction temperature and promoter composition varied [97]. These findings underscore the significant influence of reaction temperature and promoter type on light olefin production.

The choice of catalyst support, promoter, synthesis method, and process conditions play a crucial role in shaping the FTS process. The selection of an appropriate support is essential to facilitate a favorable interaction with the active metal and promoters, while ensuring caution to prevent catalyst poisoning. Incorporating alkali metals as promoters can enhance the basicity of the catalyst, thereby strengthening syngas hydrogenation. Strongly basic sites offer improved dissociative

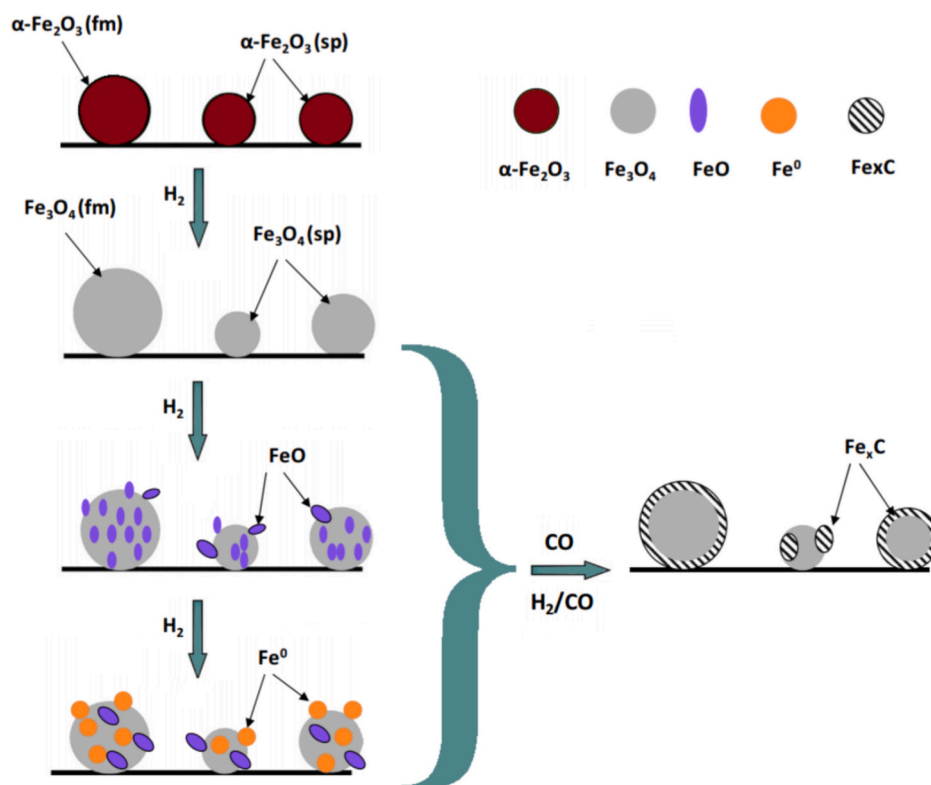


Fig. 4. Reduction and carburization behaviours of an iron-based catalyst [96].

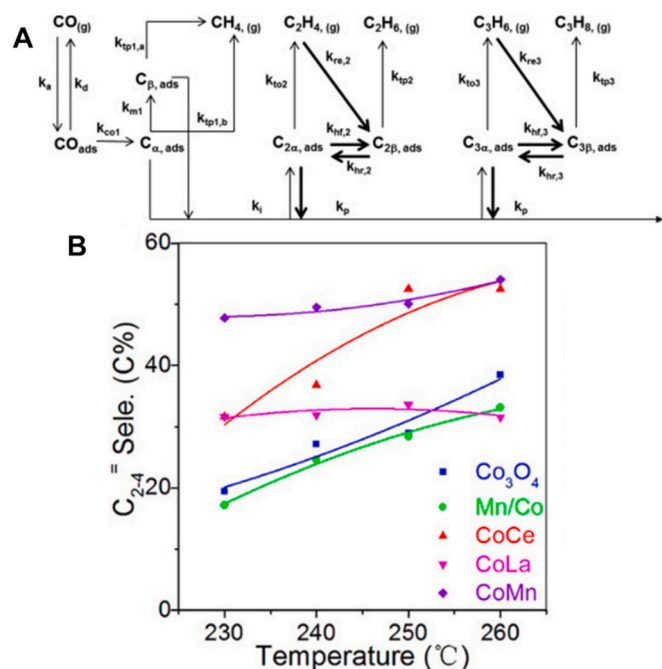


Fig. 5. (A) a schematic diagram of the mechanistic model includes the direct re-adsorption of olefins and features two surface intermediates. Adapted from [98]. (B) Selectivity of C₂-C₄ olefins for various FTO catalysts at different temperatures, 1 bar pressure, 3000 mL/(h·g_{cat}) flow rate, and H₂/CO mole ratio of 2. Adapted with permission from [97]. Copyright 2019 American Chemical Society.

adsorption of CO, leading to higher olefin selectivity compared to medium basic sites. The addition of alkali metal promoters can also influence the phase transition in catalyst reducibility, inhibiting low-temperature reduction while enhancing high-temperature reduction. Additionally, surface modifications of Fe catalysts supported on carbon materials with nitrogen-containing functionalities have shown potential in increasing light olefin selectivity in the FTS process [85]. In a recent study, the influence of alkali metal promoters (Li, Na, and K) on the performance of an iron catalyst supported on carbon nanotubes for FTS was investigated [99]. The addition of alkali metal promoters was found to impact the catalyst's crystallite size, leading to a decrease in surface area. Increasing the amount of Na and K in the catalyst resulted in a higher olefin/paraffin ratio and the formation of long-chain hydrocarbons [99].

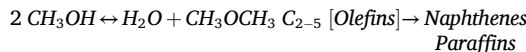
In addition, the basicity and dispersion of the metals over support influence the catalytic behaviour of metals. Supports for FT catalysts include activated carbon, alumina, silica, and titania [92,101,102]. Small cobalt particles with higher oxidation state, stronger metal-support interaction, and less aggregation of particles on the support have been reported to suppress heavy hydrocarbons formation, and increase light olefin selectivity [101]. It was also reported that a larger pore size for a Fe/SBA-15 catalyst could promote higher Fischer-Tropsch reaction rates, higher olefin and C₅+ selectivity due to easier iron carburization [92]. Multi-walled carbon nanotubes (MWCNTs) show great promise for FTS due to their exceptional mechanical properties, abundant active sites, and absence of micropores, which reduces intraparticle mass transfer limitations [103]. As a mechanically stable and inert support, alumina offers a suitable platform for investigating the interaction between promoters and iron active sites [85]. Additionally, the dispersion of active sites on silica supports is influenced by the type, concentration, and distribution of silanol groups on the silica surface, ultimately impacting the catalytic activity. Table 3 presents the results of catalytic FTS of CO and H₂ for the production of light olefins, utilizing various catalysts and conditions.

3.2. Indirect Processes of light olefins from syngas

There are different indirect processes to convert syngas to light olefins. The syngas-to-Fischer-Tropsch liquids (FTL) followed by catalytic cracking pathway is a well-established, commercially proven process that offers greater product flexibility, including the production of fuels (e.g., diesel) and chemicals [112]. However, it involves higher energy consumption and lower olefin selectivity due to the additional cracking step required [112]. The choice between these processes depends on whether the goal is to maximize olefin production or to produce a broader range of hydrocarbons. Another indirect process involves converting syngas to light olefins via lower alcohol synthesis and dehydration, or via the conversion of syngas to DME, which is then dehydrated to olefins. These pathways provide alternatives to direct syngas-to-olefins processes and are similar to the MTO process.

Given the limited selectivity of the FTS reaction in producing light olefins, researchers have directed their focus towards exploring alternative routes to produce these olefins from C₁ sources. This led to a breakthrough in C₁ chemistry in 1977 when scientists at the Mobil Oil Corporation (currently ExxonMobil) discovered that methanol can be converted to primarily gasoline-fraction hydrocarbons over a ZSM-5 catalyst [113–115]. This discovery quickly caught the attention of scientists in industry and academia. Early mechanistic studies revealed that methanol is first dehydrated to dimethyl ether, which is subsequently dehydrated to light olefins that then oligomerize to form mainly C₆-C₁₀ hydrocarbons [114].

Aromatics



The discovery that light olefins are formed as intermediates in the methanol-to-gasoline (MTG) reaction sparked significant interest in the potential of converting methanol into light olefins. Researchers at the Mobil Oil Corporation were successful in producing predominantly light olefins from methanol utilizing a ZSM-5 catalyst, by carefully optimizing reaction conditions, including temperature and contact time. This novel pathway came to be known as the methanol-to-olefin (MTO) route. Fig. 6 depicts the progression of reaction products during the Methanol-to-Gasoline (MTG) reaction using a ZSM-5 catalyst at 371 °C and 1 bar, tracked throughout the reaction duration. Initial mechanistic investigations of the MTG process revealed that by modifying the reaction conditions, it is possible to “interrupt” the process, favouring the production of light olefins rather than hydrocarbons typically found in the gasoline fraction [115].

To this end, researchers at Union Carbide announced in 1981 that they had developed a novel silicoaluminophosphate zeolite, SAPO-34, with exceptional selectivity towards light olefins [114]. The outstanding performance of this novel SAPO-34 catalyst for the MTO reaction was attributed to primarily two factors. The first is the relatively smaller pore size of SAPO-34 compared to ZSM-5. This provides SAPO-34 with excellent shape-selectivity that minimizes or prevents the formation of branched and long-chain hydrocarbons, as well as the outward diffusion of aromatics [114]. The second factor is the relatively milder acidity of SAPO-34 compared to ZSM-5. The lower acidity of SAPO-34 reduces the extent of hydrogen transfer reactions, which maximizes the yields of olefins and minimizes that of paraffins [114].

The remarkable success of the MTO process at the lab and pilot-scale in the early 1980s generated more interests for its commercialization, particularly in China, where large amounts of coal reserves are present, but not much oil and gas. This led to the formation of a research division solely focusing on MTO research in the Dalian Institute of Chemical Physics (DICP) in 1982 [113]. Almost 30 years of research efforts with several successful pilot demonstrations by DICP culminated in the world's first commercial MTO plant in China in 2010 [113,114].

Depending on the technology employed, commercial MTO reactions take place within a temperature range of 300–500 °C, and a pressure

Table 3
Catalytic FTS of syngas to light olefin production.

Feedstock	Reactor	Condition	Catalyst	Product yield (mol%), CO ₂ free	Remarks	Year and reference
CO and H ₂ (1:1)	Fixed-bed microreactor	300 °C, 1 bar, 4.2 L h ⁻¹ g _{cat} ⁻¹	Fe-K/Nitrogen-doped CNTs (2, 5, 8, 10, 12, and 15 wt% Fe)	10 % Fe catalyst (highest olefin yield): 17.3 % CH ₄ , 54.6 % C ₂ -C ₄ olefins, 5.9 % C ₂ -C ₄ alkane, 22.2 % C ₅₊	16.5 % CO conversion, 23.6 % CO ₂ selectivity from CO	2014 [104]
CO and H ₂ (1:1)	Fixed-bed reactor	270 °C, 20 bar, 30 L h ⁻¹ g _{cat} ⁻¹	Fe/Mn _{17.0} K _{3.0} - CNTs	17.2 % CH ₄ , 51.7 % C ₂ -C ₄ olefins, 9.0 % C ₂ -C ₄ alkane, 22.1 % C ₅₊	30.1 % CO conversion, 66.0 % hydrocarbon selectivity	2018 [105]
CO and H ₂ (1:1)	Fixed-bed reactor	300 °C, 10 bar, 5 g _{cat} h mol ⁻¹	FeMn/S80-E (Ethylene glycol pretreated silica support)	13.3 % CH ₄ , 54.6 % C ₂ -C ₄ olefins, 11.7 % C ₂ -C ₄ alkane, 20.4 % C ₅₊	50.5 % CO conversion, 33.4 % CO ₂ selectivity from CO	2015 [106]
CO and H ₂ (1:1)	16 parallel milli-fixed-bed reactors	350 °C, 1 bar, GHSV = 3.4 L h ⁻¹ g _{cat} ⁻¹	FeBi/SiO ₂	29 % CH ₄ , 53 % C ₂ -C ₄ olefins, 8 % C ₂ -C ₄ alkane, 10 % C ₅₊	17 % CO conversion, 48 % CO ₂ selectivity from CO	2017 [100]
CO and H ₂ (1:1)	16 parallel milli-fixed-bed reactors	350 °C, 10 bar, GHSV = 3.4 L h ⁻¹ g _{cat} ⁻¹	FeBi/SiO ₂	24 % CH ₄ , 26 % C ₂ -C ₄ olefins, 21 % C ₂ -C ₄ alkane, 29 % C ₅₊	70 % CO conversion, 49 % CO ₂ selectivity from CO	2017 [100]
CO and H ₂ (1:2)	Fixed-bed reactor	300 °C, 20 bar, GHSV = 1.5 L h ⁻¹ g _{cat} ⁻¹	Fe-Mn-Cu/SiO ₂	20.0 % CH ₄ , 40.1 % C ₂ -C ₄ olefins, 30.4 % C ₂ -C ₄ alkane, 9.5 % C ₅₊	70 % CO conversion, 49 % CO ₂ selectivity from CO	2018 [107]
CO and H ₂ (1:1)	Fixed-bed reactor	340 °C, 20 bar, GHSV = 3 L h ⁻¹ g _{cat} ⁻¹	Fe-S-Na/α-Al ₂ O ₃	16 % CH ₄ , 49 % C ₂ -C ₄ olefins, 7 % C ₂ -C ₄ alkane, 21 % C ₅₊	60–66 % CO conversion, 45–50 % CO ₂ selectivity from CO	2013 [108]
CO and H ₂ (1:2.7)	Fixed-bed reactor	350 °C, 20 bar, GHSV = 3 L h ⁻¹ g _{cat} ⁻¹	Fe/Na/Zn	25.60 % CH ₄ , 53.32 % C ₂ -C ₄ olefins, 7.72 % C ₂ -C ₄ alkane, 13.36 % C ₅₊	95.09 % CO conversion, 15.79 % CO ₂ selectivity from CO	2018 [109]
CO and H ₂ (1:1.1)	Fixed-bed reactor	340 °C, 10 bar, GHSV = 7.4 L h ⁻¹ g _{cat} ⁻¹	1Ag10Fe/MnOx (1 wt% Ag, 10 wt% Fe)	25.1 % CH ₄ , 35.4 % C ₂ -C ₄ olefins, 13.6 % C ₂ -C ₄ alkane, 25.8 % C ₅₊	50.3 % CO conversion, 45.6 % CO ₂ selectivity from CO	2018 [110]
CO and H ₂ (1:1)	Fixed-bed reactor	280 °C, 10 bar, 5 g _{cat} h mol ⁻¹	Fe-Zr	18.0 % CH ₄ , 57.0 % C ₂ -C ₄ olefins, 12.3 % C ₂ -C ₄ alkane, 12.7 % C ₅₊	40.6 % CO conversion, 39.7 % CO ₂ selectivity from CO	2019 [111]
CO and H ₂ (1:1.1)	Fixed-bed reactor	300 °C, 10 bar, GHSV = 2.2 L h ⁻¹ g _{cat} ⁻¹	Fe/(6 wt% C)SiO ₂	17.2 % CH ₄ , 24.7 % C ₂ -C ₄ olefins, 16.1 % C ₂ -C ₄ alkane, 41.9 % C ₅₊	51.4 % CO conversion, 40.2 % CO ₂ selectivity from CO	2017 [93]
CO and H ₂ (1:1.1)	Fixed-bed reactor	300 °C, 10 bar, GHSV = 2.2 L h ⁻¹ g _{cat} ⁻¹	Fe3.2 K0.1S/(6 wt% C) SiO ₂	16.0 % CH ₄ , 51.7 % C ₂ -C ₄ olefins, 11.8 % C ₂ -C ₄ alkane, 20.4 % C ₅₊	11.8 % CO conversion, 48.7 % CO ₂ selectivity from CO	2017 [93]

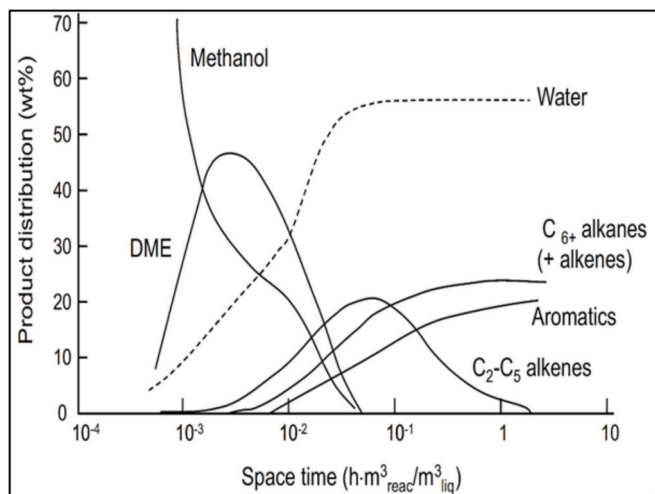


Fig. 6. Evolution of the reaction products during methanol-to-gasoline [MTG] reactions over a ZSM-5 catalyst at 371 °C and 1 bar over the course of the reaction [115].

range of 1–3 bar over a SAPO-34 catalyst. There are currently four commercial MTO technologies on the market: D-MTO/-MTO-II, S-MTO, MTO by UOP/Norsk Hydro, and MTP by Lurgi [113–115]. All of them utilize a fluidized bed reactor due to the relatively fast deactivation of the catalyst. Table 4 presents a summary for each of these MTO technologies.

The direct conversion of methanol to light olefins has ignited

Table 4
Current Commercial MTO Technology Providers [113–115].

Technology	Remarks
D-MTO/-MTO-II	D-MTO/-MTO-II stands for dimethyl ether/methanol to olefins (DMTO) and methanol to olefins (MTO). This technology was co-developed by DICP and Sinopec. As of 2019, it had the largest share in China in term of units (64 %) and capacity (70 %). Reaction conditions are in the range of 400–500 °C and 4–5 bar. The process utilizes a fluidized bed reactor, catalyst regenerator and separation units.
S-MTO	This technology was developed by Sinopec. It is similar to DMTO/MTO-II. The essential difference is that S-MTO employs a novel and patented version of the SAPO-34 catalyst that is capable to alter the ratio of ethylene/propylene from 0.6 to 1.3 based on reaction conditions.
UOP/ Norsk Hydro	This MTO technology was developed by UOP and the Norwegian-based Norsk Hydro. In this process, methanol is first preheated to the gas phase and then sent to the MTO reactor. Reaction conditions are in the range of 400–550 °C and 1–4 bar. The conversion of methanol is almost 100 %, and the selectivity of the catalyst to ethylene and propylene is about 80 %. Heavier olefins formed (C ₄ -C ₆) are cracked in a cracking unit into light olefins. The methanol to propylene (MTP) technology was developed by Lurgi. As the name suggests, it is highly selective towards propylene (over 99 %). During the Lurgi process, methanol is converted to the gas phase at around 260 °C. It is then sent to a dimethyl ether reactor, where it is dehydrated to dimethyl ether. Around 75 % of methanol is converted to dimethyl ether, as a result. The dimethyl ether and unreacted methanol mixture are then heated to around 470 °C and sent to the first MTP reactor, where steam is also introduced. The first MTP reactor converts more than 99 % of the reaction mixture to propylene. A second and third reactors are used to maximize propylene yield.
MTP	

significant interest in elucidating the underlying chemistry of the MTO reaction [113]. It has been observed that during the induction period of the MTO reaction, the formation of minute product quantities results in considerably higher methanol conversion at later stages, indicating an autocatalytic nature of the reaction [113,116]. Furthermore, the reaction pathway during the induction period involves relatively high activation energy, particularly in the formation of the first carbon-carbon (C—C) bond [113,116].

The mechanism responsible for the formation of the first C—C bond has been a subject of substantial debate in the literature, with several proposed mechanisms, including the oxysonium ylide mechanism, carbocation mechanism, free-radical mechanism, and carbene mechanism [113,116–119]. While initial hypotheses suggested that impurities and traces from reactants and/or carrier gas might be responsible for the first C—C bond formation, subsequent studies conducted by Hunger and co-workers refuted this hypothesis, showing no significant effect on the process [113,116–119]. Building on this understanding of fundamental mechanisms, Fig. 7A illustrates a practical route: the synthesis of C₂–C₄ olefins from syngas through a two-step process: syngas-to-methanol (methanol synthesis) followed by methanol-to-olefins conversion [120]. The use of methanol as an intermediate in the transformation of syngas into olefins offers improved energy and cost efficiency. Furthermore, product selectivity can be optimized by leveraging the shape-selective properties of molecular sieves.

Fig. 7B and C illustrate the influence of total syngas pressure and temperature on the catalytic performance of the Zn–ZrO₂/SSZ-13 catalyst at 673 K and an H₂/CO ratio of 2 [120]. Upon increasing the pressure of syngas, the conversion of CO increased significantly but the selectivity of C₂–C₄ olefins decreased. Thus, there exists an optimum total pressure for the conversion of syngas into light olefins [120]. At temperatures below 600 K, CH₃OH/DME are the predominant products, indicating that the zeolite-catalyzed C—C coupling of CH₃OH/DME requires higher temperatures to proceed. As the reaction temperature increases, the selectivity for C₂–C₄ olefins rises at the expense of CH₃OH/DME. Specifically, at 673 K, the selectivity for C₂–C₄ olefin selectivity and the CO conversion increased to 75 % and 23 %, respectively

However, further temperature increases lead to a decline in C₂–C₄ olefin selectivity and a rise in of C₂–C₄ paraffin selectivity, attributed to the hydrogenation of light olefins [120].

Recent studies employing advanced analytical techniques, such as solid-state Nuclear Magnetic Resonance (NMR) spectroscopy, Diffuse Reflectance Infrared Fourier Transform Spectroscopy (DRIFTS), and Gas Chromatography-Mass Spectrometry (GC–MS), have provided evidence that surface-methoxy-species (SMS) are formed on Brønsted acid sites during the induction period of the MTO reaction. Based on these findings, it is now widely believed that these SMS species react with adsorbed methanol and/or dimethyl ether to form the first C—C bond [117–119].

Several indirect routes explaining the formation of olefins from methanol were proposed in the 1980s and 1990s. Dassau and co-workers suggested the alkene-based route, while Mole and co-workers reported the significant role of aromatics in the formation of olefins during the MTO reaction [71,121]. Additionally, in 1993, Dahl and Kolboe proposed the Hydrocarbon Pool (HCP) mechanism, which involves the formation of various aromatic species (HCP species) confined in the zeolite cage [118,119,121]. According to their proposal, these HCP species act as co-catalysts for the synthesis of C₂–C₄ olefins from methanol [113,118,119,121].

Numerous studies have been conducted to investigate the Hydrocarbon Pool (HCP) mechanism since its proposal, and many of these studies have reported a strong correlation between the formation of methylbenzene species and the generation of olefins over eight-membered ring zeolite catalysts [113]. For instance, using solid-state NMR, Xu and White detected the presence of carbenium ions, such as heptamethylcyclopentenyl cations, when the MTO reaction was catalyzed by SAPO-34, and heptamethylbenzenium cations when catalyzed by H-β-zeolite [113]. Over a ZSM-5 zeolite, HCP species like 1,3-dimethylcyclopentadienyl and 1,1,2,4,6-pentamethylbenzenium cations were detected, leading to the proposal of a dual-cycle mechanism to account for the relatively wide product distribution observed over these types of zeolites [113,122]. Specifically, it was suggested that over ZSM-5 catalysts, the generation of ethylene follows the HCP mechanism,

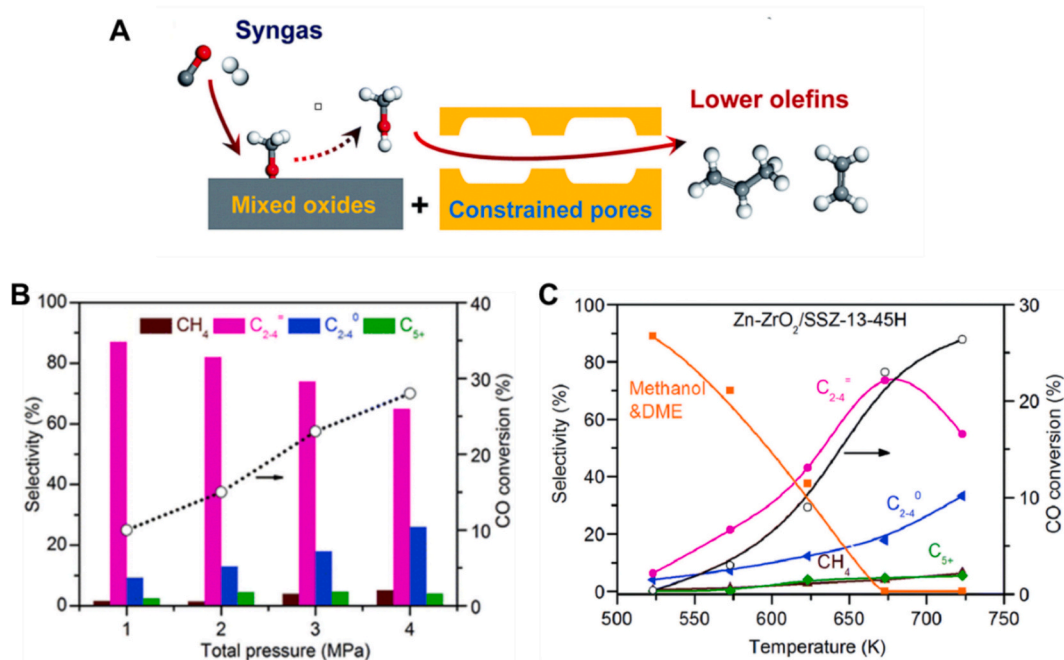


Fig. 7. (A) the process to produce light olefins from syngas through a methanol intermediate (B) the influence of total syngas pressure on the catalytic activity of the Zn–ZrO₂/SSZ-13-45H catalyst; (C) the catalytic performance of Zn–ZrO₂/SSZ-13-45H catalysts during syngas conversion at various temperatures. The reaction conditions: a catalyst mass of 0.60 g, H₂/CO mole ratio of 2:1, temperature of 673 K, flow rate of 30 mL min⁻¹, and a reaction duration of 10 h. Adapted from [120], with permission from the Royal Society of Chemistry.

while the formation of propylene and higher olefins proceeds through the alkene-based mechanism [113]. As a result, researchers at the DICP investigated the effect of cofeeding ethylene with methanol during the MTO reaction over different zeolite catalysts. They concluded that the HCP mechanism dominates the MTO reaction only over optimized acidic catalysts and is inactive over weakly acidic catalysts. In contrast, alkene methylation and cracking routes become the dominant pathways over catalysts with weak acidity [113].

Catalyst deactivation during the MTO reaction has also been the subject of extensive research. It occurs due to the formation of coke species, which can either poison the acidic active sites of the catalyst or block the access of methanol to these sites. Haw and coworkers reported that over a SAPO-34 catalyst, methylbenzene species formed as a result of the HCP mechanism were gradually converted during the reaction to methylnaphthalenes, polyaromatics, phenanthrene derivatives, and pyrene [123]. This conversion process led to a severe reduction in mass transport rates to and from the zeolite cage, thereby deactivating the catalyst. Additionally, researchers at the DICP observed a sharp decrease in methanol conversion over a SAPO-34 catalyst at around 350 °C compared to conversions at 325 °C and 400 °C [113]. Fig. 8 shows the distribution of effluent in a fluidized-bed methanol conversion process during a programmed temperature increase [113]. Further investigation revealed that inactive diamondoid hydrocarbons, such as polymethyladamantanes, formed within the zeolite cage at temperatures between 325 °C and 350 °C, in addition to benzenium ions. As the temperature was increased to 400 °C, the previously inactive polymethyladamantanes species converted into methylnaphthalenes and polyaromatics. This conversion process led to a partial recovery in catalyst activity at 400 °C [113].

Apart from acidity, the type of ring, cavity structure, and topology of the zeolite employed during the MTO reaction significantly influence the obtained product distribution [113,114,124]. It has been reported that these parameters have an impact on the type of HCP species formed, subsequently affecting the product distribution [113,124]. For instance, Liu and colleagues reported that over SAPO-35 (LEV cavity, $6.3 \times 7.3 \text{ \AA}$), ethylene was the dominant product, while both ethylene and propylene were the dominant products over SAPO-34 (CHA cavity, $6.7 \times 10 \text{ \AA}$), and butenes were the dominant products over DNL-6 (CHA cavity, 11.4

$\times 11.4 \text{ \AA}$) [114,125,126].

Several studies have investigated the single-step conversion of synthesis gas to light olefins by combining a metal oxide catalyst with a zeolite catalyst. The oxide catalyst promotes the hydrogenation of CO, while the zeolite catalyst facilitates C–C coupling. In one study, Jiao et al. [14] achieved a selectivity of 80 % towards light olefins at a 17 % CO conversion over a ZnCrO_x /mesoporous SAPO zeolite (MSAPO) catalyst, which exhibited excellent stability for up to 100 h. In the same study, Bao and co-workers examined the effect of different bed configurations on the selectivity of light olefins. Four bed configurations were tested: (1) only ZnCrO_x catalyst bed, (2) two separate beds composed of the ZnCrO_x catalyst in the upper bed and MSAPO catalyst in the lower bed, (3) alternating thin beds composed of ZnCrO_x and MSAPO catalysts, and (4) a thoroughly mixed bed composed of ZnCrO_x and MSAPO catalysts. The highest selectivity towards light olefins was achieved over the thoroughly mixed bed configuration, while the bed that contained only ZnCrO_x showed the highest selectivity towards methane. The group also reported that higher olefin selectivity is obtained as the space velocity is increased. The authors attributed the high light olefins selectivity obtained at high space velocity and over the thoroughly mixed bed to the relatively fast transport of the reaction intermediates formed in the oxide layer to the zeolite catalyst. Lower space velocities and lack of proximity between the oxide and zeolite layers facilitate the hydrogenation of the intermediates to methane on the oxide layer and/or in the gas phase before reaching the zeolite catalyst [14].

In addition, Wang and co-workers investigated several combinations of metal oxides and SAPO-34 for the direct conversion of synthesis gas to light olefins. The highest light olefins selectivity (74 %) was obtained over a Zr-Zn/SAPO-34 catalyst [127]. Furthermore, Liu and co-workers reported a 77 % selectivity towards $\text{C}_2\text{-C}_4$ olefins at a CO conversion of approximately 7 % over a ZnAlO_x /SAPO-34 catalyst [128]. The group also investigated the effect of different mixing techniques of the ZnAlO_x and SAPO-34 on the product distribution. Three different ways of testing the ZnAlO_x and SAPO-34 catalysts were used: (1) granules of ZnAlO_x and SAPO-34 mixing, (2) ZnAlO_x and SAPO-34 grinding in an agate mortar, (3) dual-bed composed of ZnAlO_x in the upper bed and SAPO-34 in the lower bed. The light olefin selectivity was close in all three tests, with the highest selectivity observed in the dual-bed configuration. A fourth

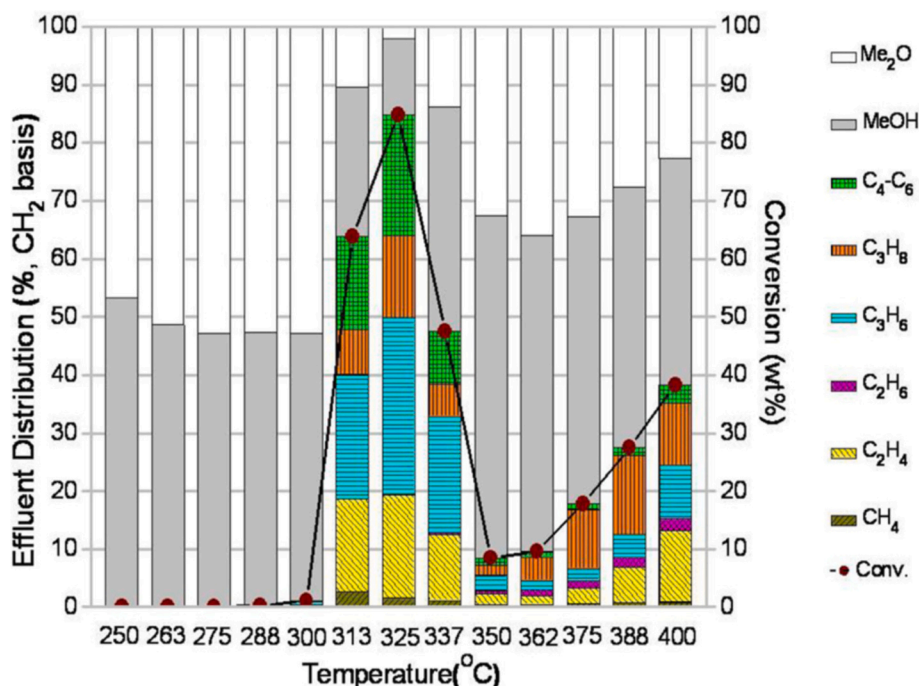


Fig. 8. Effect of reaction temperature on the product distribution during the MTO reaction [113].

catalytic test that involved only ZnAlO_x showed very high selectivity towards dimethyl ether and CO_2 . The authors attributed this to the promotion of the oxide layer for the hydrogenation of CO and the water-gas shift reaction. They also suggested that the low dimethyl ether selectivity in the tests that combined both ZnAlO_x and SAPO-34 implies that the hydrocarbons produced in these tests mainly originated from the conversion of dimethyl ether [128].

Commercial MTO technologies offer significant advantages in industrial applications, including feedstock flexibility, as methanol can be sourced from coal, natural gas, or biomass. MTO processes exhibit high selectivity for light olefins, particularly ethylene and propylene. When methanol is derived from renewable sources, MTO can contribute to a lower carbon footprint compared to traditional naphtha cracking. However, several challenges remain in industrial use, including catalyst deactivation, the energy-intensive nature of methanol production from syngas, and the need for a stable, economically viable methanol supply chain for MTO processes using waste and biomass feedstocks [33,113]. These factors make the process vulnerable to changes in prices and interruptions in supply.

4. Current trends and perspectives

As explained in the Introduction section, the contemporary landscape of light olefin production is marked by rapid advancements driven not only by the escalating demand for critical petrochemical components but also by a burgeoning impetus towards sustainability. In response to global concerns regarding environmental impact and resource depletion, researchers and industries are actively exploring alternative and more sustainable feedstocks for the synthesis of light olefins [10,11,57]. The utilization of renewable and abundant biomass resources provides a pathway towards a more environmentally friendly and sustainable future for light olefin synthesis. This section scrutinizes the present trends and perspectives in the realm of light olefin manufacturing from biomass and waste. It encompasses advanced catalyst design, considerations in reaction engineering, mechanistic elucidation, commercialization endeavours, technical challenges, prevailing market trends, sustainability, policy support, collaboration and research, and other pivotal factors.

4.1. Advanced catalyst design

In FTS-based and OX-ZEO catalytic processes, research is focussing on studying how the addition of promoters and the customization of zeolite structures through precise modifications can enhance performance. These adjustments involve variations in attributes such as acidity, porosity, and channel dimensions to fine-tune zeolites for specific applications. In some studies, La-modified HZSM-5 catalysts were employed to improve the selectivity of light olefins from bio-oil and biomass, while catalysts modified with Mg demonstrate enhancements in both selectivity and stability [53,69,129]. In FTS processes, where Fe and Co are the predominantly used catalysts, current research towards the synthesis of light olefins is focusing on the effects of metal support interaction [92,101,102], alongside investigating catalyst deactivation and the poisoning effects of sulfur [130,131], nitrogen [131,132], and alkali metals [133,134] on these catalysts. For biomass and waste resources, more resilient catalysts are required that can withstand the deleterious effects of contaminants, as well as integration with processes at smaller scale, which is typical of distributed nature of feedstock. Additionally, interest is growing in exploring nano-engineered catalysts to enhance selectivity and yield of light olefins. An innovative approach involves the creation of hybrid catalysts, which combine different components to leverage their unique strengths, but also obtain new synergies. For example catalysts that combine metal oxides with zeolites within the same particle/pellet could demonstrate promising selectivity for light olefins.

4.2. Mechanistic insights

Unravelling the mechanisms underlying olefin production reactions forms the bedrock for informed catalyst design and process optimization. Mechanistic inquiries should extend to include catalyst deactivation, as poisons and coke species accumulate over time, diminishing catalyst activity and selectivity. For example, recent studies have afforded insights into the formation of surface-methoxy-species (SMS) on Brønsted acid sites during the MTO reaction, and the Hydrocarbon Pool (HCP) mechanism with zeolite catalysts [135,136]. Notably, systems such as the dual-bed STO catalyst ($\text{ZnAlO}_x/\text{SAPO-34}$) [137] and $\text{CuZnAlO}_x + \text{ZSM-5}$ [138] demonstrate high syngas conversion to olefins with lower CO_2 emissions. For most of the olefin synthesis processes, a systematic understanding of deactivation mechanisms is indispensable for the formulation of strategies aimed at mitigating coke formation and extending catalyst lifetime.

4.3. Commercialization and technical challenges

Steadily growing global demand for light olefins, notably ethylene and propylene requires more sustainable manufacturing routes. Consequently, the integration of renewable feedstocks emerges as a strategic solution to mitigate greenhouse gas emissions and diminish dependence on fossil fuels [139]. However, this transition is fraught with technical challenges, especially in the context of biomass and waste-based operations. A case in point pertains to the gasification technology utilized in syngas production. One technical impediment lies with those gasification plants, where the dearth of waste-fuelled gasifiers capable of producing clean syngas underscores a substantial technological deficit. Despite these hurdles, there is growing interest among researchers and industrial practitioners to assimilate biomass within downstream processes. This strategic orientation seeks not only to maximize feedstock efficiency but also to curtail waste generation. Furthermore, the paradigm of integrated biorefineries, envisioned to concurrently produce chemicals and biofuels, is progressively gaining acceptance [23]. However, realizing this potential is inextricably linked to overcoming challenges, such as those associated with clean syngas production from waste-fuelled gasifiers [73,140]. Consequently, while the momentum towards biomass integration and sustainable production methodologies is commendable, it necessitates a concerted effort to address and surmount these technical barriers.

4.4. Biomass availability and competition

Evaluating the accessibility of biomass feedstocks and their potential competition with alternative uses like biofuels and bioenergy becomes exceptionally significant. Sourcing biomass wisely and using it efficiently are essential prerequisites. Here, it is crucial to acknowledge the challenges and downsides associated with biomass utilization for chemical and fuel production [23]. These challenges encompass issues such as competition for arable land, which may also be needed for food production, and the potential for deforestation, which has adverse effects on ecosystems and biodiversity [27]. Choice of second or third generation biomass is more complex, but preferred.

4.5. Techno-economic analysis

A crucial aspect of viable biomass-to-olefin production research is conducting techno-economic analyses of different conversion pathways. These analyses assess the economic feasibility, production costs, and potential profitability of various biomass-to-olefin processes [23]. For instance, recent studies comparing the hydrophobic FeMn@Si-c catalyst with the traditional hydrophilic FeMn@Si catalyst in a 2.87 Mt./y coal-to-olefin plant have demonstrated that the hydrophobic FeMn@Si-c catalyst offers significant economic and environmental advantages [141]. This suggests a strong potential for industrial application in

producing C₂-C₄ olefins from coal-based syngas. Understanding the economics of these processes is crucial for attracting investment and facilitating the scale-up of production, ensuring the commercial viability of biomass-to-olefin technologies.

4.6. Sustainability

The future of biomass and waste to olefin production resides in a sustainable development framework that addresses environmental, social, and economic facets. Researchers have evaluated olefin feedstock alternatives through Life Cycle Analysis (LCA), indicating that renewable feedstocks can significantly reduce greenhouse gas emissions and reliance on fossil fuels [75,142]. Comparing LCAs of emerging bio-based products to their fossil-based counterparts reveals significant potential for the bio-economy to reduce greenhouse gas emissions: it is reported that reductions in greenhouse gas emissions for biorefinery products could generally be 73 % [143]. Although various methods exist to reduce the carbon footprint of olefin production, traditional fossil-based olefins from the naphtha-based steam cracking process are projected to dominate the market for the next 20 to 30 years [144]. Transitioning to green feedstocks could decrease CO₂ emissions by up to 45 %, but broader adoption may face economic challenges compared to conventional routes [144]. The proportion of “green” olefins is expected to increase over the coming decades, though substantial advancements in biomass gasification or lignocellulosic bio-oil upgrading are necessary. Carbon pricing and regulatory measures can make bio-based olefins more competitive by narrowing the cost gap with fossil-based production. By attaching a financial cost to emissions, carbon pricing and incentives like subsidies, tax breaks, and carbon credits can enhance the economic viability of bio-based olefins. This could drive the industry to adopt lower-carbon feedstocks and accelerate the transition to renewable olefin production through mechanisms such as carbon taxes and emission trading systems. Plastic waste recycling, while not significantly reducing carbon emissions, could lower fossil feedstock use by 25 to 55 % [144]. Light olefins produced from plastic waste are likely to see significant growth due to strong industry commitments, since this technology could possibly achieve emission reductions of 80–90 %, though these are currently not economically viable without carbon taxes and government incentives [144]. A comparative analysis revealed that the Global Warming Potential (GWP) of olefins from solid waste exceeds that from wood, due to lower feedstock quality and high energy demands for the mechanical treatment of MSW [142]. Researchers found that using primary biomass for syngas production reduces Global Warming Impact (GWI) compared to CO₂ and steel mill flue gases, but increases freshwater eutrophication and land use, which can be mitigated by switching to bio-waste as feedstock [145]. Second and third-generation biomass sources, including agricultural residues and algae, are viewed as more environmentally sustainable because they have a lower impact on food crop competition and demand for arable land [146].

Comprehensive evaluations should include LCA to fully understand the environmental impacts and resource utilization of various production methods. Ultimately, a combination of strategies, including biomass utilization, increased recycling rates, low carbon electrification of the industry, and reduced product demand, will be required to achieve net-zero emissions in the chemical and plastic industries [143]. Systemic effects of changing production pathways, utility and emission allocation between industry sectors and resource availability limitations necessitate a system-based evaluation, should be explored in further research [142].

4.7. Policy support

Government policies and incentives in some regions are promoting the development of the biomass-to-olefin industry. This support includes subsidies, tax incentives, and renewable energy mandates, which can

influence the allocation of biomass resources and project viability [23,147].

4.8. Collaboration and research

Collaboration between academia, industry, and government research agencies continues to drive innovation in biomass-to-olefin production. Research efforts are ongoing to improve process efficiency, reduce costs, and address sustainability concerns, but this is unlikely to have substantial impact unless there is dialogue, or, preferably, co-creation and co-design with stakeholders, and policy makers, to open routes for sustainable development in every sense [84].

5. Conclusions

Although light olefins are typically found as gaseous byproducts in thermochemical processes, such as pyrolysis and gasification, they are considered secondary products, and only few studies have focused on their production compared to other products. Direct pyrolysis of biomass and waste exhibits relatively low efficiency in terms of light olefin production but results in a high content of bio-oil, which can be further converted into light olefins through catalytic cracking. The conversion of bio-oil involves reactions such as decarbonylation, decarboxylation, dehydration, oligomerization, isomerization, and dehydrogenation, which also generate CO, CO₂, and H₂O to remove oxygen. The main challenge in catalytic cracking of biomass pyrolysis vapours or bio-oil is coke formation and other forms of catalyst deactivation. The rapid formation of coke competes with olefin and aromatic production, and it deactivates the catalyst. Overcoming deactivation is crucial for biomass-based refineries to compete with conventional refineries that use fossil fuels. Further research is needed to design and implement new units for upgrading raw bio-oil and its mixture with other oxygenates within the scope of the petrochemical industry.

Gasification offers some advantages compared to pyrolysis, such as higher scalability, process efficiency and feedstock flexibility. Despite a minor quantity of light olefins in produced in gasification, the main product is syngas, that, once cleaned, can be used as a chemical feedstock for subsequent olefins synthesis.

The production of light olefins using syngas as a feedstock through FTS is significant. Iron and cobalt are the typical catalysts in FTS. Iron is more tolerant of sulfur impurities, less expensive, and more selective towards light olefins, while cobalt-based catalysts are highly active, exhibit low WGS activity (requiring higher H₂/CO ratios), and demonstrate superior stability. Process conditions, catalyst support, promoter usage, and synthesis methods can all influence process performance. The addition of alkali metals can enhance the basicity of the catalyst, leading to stronger active sites for syngas hydrogenation. These highly basic sites promote better dissociative adsorption of CO and result in higher olefin selectivity compared to catalysts with medium basicity.

Recent studies on the feasibility of direct conversion of synthesis gas to olefins through the methanol/dimethyl ether route have shown promising results. However, there are several major issues that hinder its commercialization. These challenges include low CO conversion, the undesired production of CO₂, and the need to optimize light olefins selectivity in the presence of high H₂ pressure. The direct conversion of synthesis gas is complex, as it involves the integration of a series of reactions, namely methanol synthesis, methanol dehydration, water-gas shift reaction, and methanol and/or dimethyl ether to light olefins, which are normally operated under different conditions of temperature and pressure. To overcome these challenges and fully harness the potential of the direct conversion of synthesis gas to light olefins, further research is needed to unravel the precise reaction mechanisms and identify the optimal conditions and catalysts for enhanced selectivity and conversion rates. Addressing these issues will be crucial for advancing this process towards commercialization and making it a viable alternative for sustainable olefin production.

The environmental, energy efficiency, and economic aspects of all the processes for light olefin production, as well as the carbon and energy balance of the process, can be evaluated through techno-economic and lifecycle analyses. Although technologies for syngas-to-olefin production have rapidly developed in recent years, it remains necessary for governments and policymakers to support renewable olefins for their survival and promotion in the global market.

CRedit authorship contribution statement

Hualun Zhu: Writing – review & editing, Writing – original draft, Investigation, Data curation. **Mohammed Babkoo:** Writing – original draft, Investigation. **Marc-Olivier Coppens:** Writing – review & editing, Supervision. **Massimiliano Materazzi:** Writing – review & editing, Resources, Project administration, Methodology, Funding acquisition, Conceptualization.

Declaration of competing interest

The authors declare that they have no known competing financial interests or personal relationships that could have appeared to influence the work reported in this paper.

Data availability

Data will be made available on request.

Acknowledgement

The authors gratefully acknowledge the financial support from SABIC, and the Engineering and Physical Sciences Research Council (EPSRC) through the “Nature-inspired bio-Syngas Technologies for Olefins Synthesis” Grant (EP/W019221/1).

References

- [1] I. Amghizar, L.A. Vandewalle, K.M. Van Geem, G.B. Marin, New trends in olefin production, *Engineering* 3 (2017) 171–178.
- [2] M. Bender, An overview of industrial processes for the production of olefins–C4 hydrocarbons, *ChemBioEng Rev.* 1 (2014) 136–147.
- [3] J. Panda, J. Sahoo, G. Sahoo, Structure-Reactivity Relationship of Olefins as Electrophiles and Nucleophiles: Factors Influencing, 2024.
- [4] N.V. Kolesnichenko, N.N. Ezhova, Y.M. Snatenkova, Lower olefins from methane: recent advances, *Russ. Chem. Rev.* 89 (2020) 191.
- [5] V. Zacharopoulou, A.A. Lemonidou, Olefins from biomass intermediates: a review, *Catalysts* 8 (2017) 2.
- [6] H.M. Torres Galvis, K.P. de Jong, Catalysts for production of lower olefins from synthesis gas: a review, *ACS Catal.* 3 (2013) 2130–2149.
- [7] A. Analytics, Global 1-butene market: analysis by production process, application, by region, by Country (2022 Edition): market insights and forecast with impact of COVID-19 (2017–2027), in: Azoth Analytics, 2022.
- [8] Y. Gao, L. Neal, D. Ding, W. Wu, C. Baroi, A.M. Gaffney, F. Li, Recent advances in intensified ethylene production—a review, *ACS Catal.* 9 (2019) 8592–8621.
- [9] A. Agarwal, D. Sengupta, M. El-Halwagi, Sustainable process design approach for on-purpose propylene production and intensification, *ACS Sustain. Chem. Eng.* 6 (2018) 2407–2421.
- [10] N.C. Shiba, X. Liu, Y. Yao, Advances in lower olefin production over cobalt-based catalysts via the Fischer-Tropsch process, *Fuel Process. Technol.* 238 (2022) 107489.
- [11] S. Zhao, H. Li, B. Wang, X. Yang, Y. Peng, H. Du, Y. Zhang, D. Han, Z. Li, Recent advances on syngas conversion targeting light olefins, *Fuel* 321 (2022) 124124.
- [12] M. Arabiourrutia, G. Lopez, M. Artetxe, J. Alvarez, J. Bilbao, M. Olazar, Waste Tyre valorization by catalytic pyrolysis—a review, *Renew. Sust. Energ. Rev.* 129 (2020) 109932.
- [13] A. Chiericato, J.V. Ochoa, F. Cavani, Olefins from biomass, *Chem. Fuels Bio-Based Build. Blocks* (2016) 1–32.
- [14] F. Jiao, J. Li, X. Pan, J. Xiao, H. Li, H. Ma, M. Wei, Y. Pan, Z. Zhou, M. Li, Selective conversion of syngas to light olefins, *Science* 351 (2016) 1065–1068.
- [15] A. Masudi, N.W.C. Jusoh, O. Muraza, Opportunities for less-explored zeolitic materials in the syngas-to-olefins pathway over nanoarchitected catalysts: a mini review, *Catalys. Sci. Technol.* 10 (2020) 1582–1596.
- [16] T. Kan, V. Strezov, T.J. Evans, Lignocellulosic biomass pyrolysis: a review of product properties and effects of pyrolysis parameters, *Renew. Sust. Energ. Rev.* 57 (2016) 1126–1140.

- [17] H. Zhang, R. Xiao, B. Jin, G. Xiao, R. Chen, Biomass catalytic pyrolysis to produce olefins and aromatics with a physically mixed catalyst, *Bioresour. Technol.* 140 (2013) 256–262.
- [18] V.P. Aravani, H. Sun, Z. Yang, G. Liu, W. Wang, G. Anagnostopoulos, G. Syriopoulos, N.D. Charisiou, M.A. Goula, M. Kornaros, V.G. Papadakis, Agricultural and livestock sector’s residues in Greece & China: comparative qualitative and quantitative characterization for assessing their potential for biogas production, *Renew. Sust. Energ. Rev.* 154 (2022) 111821.
- [19] N. Tripathi, C.D. Hills, R.S. Singh, C.J. Atkinson, Biomass waste utilisation in low-carbon products: harnessing a major potential resource, *NPJ Clim. Atmos. Sci.* 2 (2019) 35.
- [20] M. Materazzi, A. Holt, Experimental analysis and preliminary assessment of an integrated thermochemical process for production of low-molecular weight biofuels from municipal solid waste (MSW), *Renew. Energy* 143 (2019) 663–678.
- [21] I.S.W. Association, Global Waste Management Outlook 2024: Beyond an Age of Waste, Turning Rubbish into a Resource, 2024.
- [22] V. Wegmann, Waste Management in EUROPE, 2023.
- [23] A.I. Osman, N. Mehta, A.M. Elgarahy, A. Al-Hinai, A.A.H. Al-Muhtaseb, D. W. Rooney, Conversion of biomass to biofuels and life cycle assessment: a review, *Environ. Chem. Lett.* 19 (2021) 4075–4118.
- [24] P.G.C. Nayanathara Thatsarani Pilapitiya, A.S. Ratnayake, The world of plastic waste: a review, *Clean. Mater.* 11 (2024) 100220.
- [25] P.M. Subbarao, T.C. D’Silva, K. Adlak, S. Kumar, R. Chandra, V.K. Vijay, Anaerobic digestion as a sustainable technology for efficiently utilizing biomass in the context of carbon neutrality and circular economy, *Environ. Res.* 234 (2023) 116286.
- [26] J.R. Banu, V.G. Sharmila, U. Ushani, V. Amudha, G. Kumar, Impervious and influence in the liquid fuel production from municipal plastic waste through thermo-chemical biomass conversion technologies - a review, *Sci. Total Environ.* 718 (2020) 137287.
- [27] T.G. Ambaye, M. Vaccari, A. Bonilla-Petriciolet, S. Prasad, E.D. van Hullebusch, S. Rtimi, Emerging technologies for biofuel production: a critical review on recent progress, challenges and perspectives, *J. Environ. Manag.* 290 (2021) 112627.
- [28] P.R. Bhoi, A.S. Ouedraogo, V. Soloiu, R. Quirino, Recent advances on catalysts for improving hydrocarbon compounds in bio-oil of biomass catalytic pyrolysis, *Renew. Sust. Energ. Rev.* 121 (2020) 109676.
- [29] L. Dai, N. Zhou, Y. Lv, Y. Cheng, Y. Wang, Y. Liu, K. Cobb, P. Chen, H. Lei, R. Ruan, Pyrolysis technology for plastic waste recycling: a state-of-the-art review, *Prog. Energy Combust. Sci.* 93 (2022) 101021.
- [30] M.M. Rahman, R. Liu, J. Cai, Catalytic fast pyrolysis of biomass over zeolites for high quality bio-oil—a review, *Fuel Process. Technol.* 180 (2018) 32–46.
- [31] P.S. Rezaei, H. Shafaghat, W.M.A.W. Daud, Production of green aromatics and olefins by catalytic cracking of oxygenate compounds derived from biomass pyrolysis: a review, *Appl. Catal. A Gen.* 469 (2014) 490–511.
- [32] T. Kan, V. Strezov, T. Evans, J. He, R. Kumar, Q. Lu, Catalytic pyrolysis of lignocellulosic biomass: a review of variations in process factors and system structure, *Renew. Sust. Energ. Rev.* 134 (2020) 110305.
- [33] E. Kianfar, Comparison and assessment of zeolite catalysts performance dimethyl ether and light olefins production through methanol: a review, *Rev. Inorg. Chem.* 39 (2019) 157–177.
- [34] Q. Sun, Z. Xie, J. Yu, The state-of-the-art synthetic strategies for SAPO-34 zeolite catalysts in methanol-to-olefin conversion, *Natl. Sci. Rev.* 5 (2018) 542–558.
- [35] B.O. Adelawon, G.K. Latinwo, B.E. Eboibi, O.O. Agbede, S.E. Agarry, Comparison of the slow, fast, and flash pyrolysis of recycled maize-cob biomass waste, box-benken process optimization and characterization studies for the thermal fast pyrolysis production of bio-energy, *Chem. Eng. Commun.* 209 (2022) 1246–1276.
- [36] M.U. Joardder, P. Halder, A. Rahim, N. Paul, Solar assisted fast pyrolysis: a novel approach of renewable energy production, *J. Eng.* 2014 (2014).
- [37] D. Angin, Effect of pyrolysis temperature and heating rate on biochar obtained from pyrolysis of safflower seed press cake, *Bioresour. Technol.* 128 (2013) 593–597.
- [38] J. Encinar, J. Gonzalez, J. Gonzalez, Fixed-bed pyrolysis of *Cynara cardunculus* L. Product yields and compositions, *Fuel Process. Technol.* 68 (2000) 209–222.
- [39] G. Chang, Y. Huang, J. Xie, H. Yang, H. Liu, X. Yin, C. Wu, The lignin pyrolysis composition and pyrolysis products of palm kernel shell, wheat straw, and pine sawdust, *Energy Convers. Manag.* 124 (2016) 587–597.
- [40] A.N. Amenaghawon, C.L. Anyalewechi, C.O. Okieimen, H.S. Kusuma, Biomass pyrolysis technologies for value-added products: a state-of-the-art review, *Environ. Dev. Sustain.* 23 (2021) 14324–14378.
- [41] N.S. Almuqati, A.M. Aldawsari, K.N. Alharbi, S. González-Cortés, M.F. Alotibi, F. Alzaidi, J.R. Dilworth, P.P. Edwards, catalytic production of light olefins: perspective and prospective, *Fuel* 366 (2024) 131270.
- [42] S.W. Kim, Y.T. Kim, Y.F. Tsang, J. Lee, Sustainable ethylene production: recovery from plastic waste via thermochemical processes, *Sci. Total Environ.* 903 (2023) 166789.
- [43] X. Huang, J. Ren, J.-Y. Ran, C.-L. Qin, Z.-Q. Yang, J.-P. Cao, Recent advances in pyrolysis of cellulose to value-added chemicals, *Fuel Process. Technol.* 229 (2022) 107175.
- [44] R. Liu, M.M. Rahman, M. Sarker, M. Chai, C. Li, J. Cai, A review on the catalytic pyrolysis of biomass for the bio-oil production with ZSM-5: focus on structure, *Fuel Process. Technol.* 199 (2020) 106301.
- [45] S. Du, D.P. Gamliel, J.A. Valla, G.M. Bollas, The effect of ZSM-5 catalyst support in catalytic pyrolysis of biomass and compounds abundant in pyrolysis bio-oils, *J. Anal. Appl. Pyrolysis* 122 (2016) 7–12.

- [46] D.P. Serrano, J.A. Melero, G. Morales, J. Iglesias, P. Pizarro, Progress in the design of zeolite catalysts for biomass conversion into biofuels and bio-based chemicals, *Catal. Rev.* 60 (2018) 1–70.
- [47] Q. Wang, W. Zhang, X. Ma, Y. Liu, L. Zhang, J. Zheng, Y. Wang, W. Li, B. Fan, R. Li, A highly efficient SAPO-34 catalyst for improving light olefins in methanol conversion: Insight into the role of hierarchical porosities and tailoring acid properties based on in situ NH₃-poisoning, *Fuel* 331 (2023) 125935.
- [48] S. Kelkar, C.M. Saffron, Z. Li, S.-S. Kim, T.J. Pinnavaia, D.J. Miller, R. Krieger, Aromatics from biomass pyrolysis vapour using a bifunctional mesoporous catalyst, *Green Chem.* 16 (2014) 803–812.
- [49] T. Funazukuri, R.R. Hudgins, P.L. Silveston, Production of olefins from flash pyrolysis of cellulose-containing material, *J. Anal. Appl. Pyrolysis* 17 (1989) 47–66.
- [50] T.R. Carlson, Y.-T. Cheng, J. Jae, G.W. Huber, Production of green aromatics and olefins by catalytic fast pyrolysis of wood sawdust, *Energy Environ. Sci.* 4 (2011) 145–161.
- [51] H. Zhang, R. Xiao, B. Jin, D. Shen, R. Chen, G. Xiao, Catalytic fast pyrolysis of straw biomass in an internally interconnected fluidized bed to produce aromatics and olefins: effect of different catalysts, *Bioresour. Technol.* 137 (2013) 82–87.
- [52] C. Hu, C. Liu, Q. Liu, H. Zhang, S. Wu, R. Xiao, Effects of steam to enhance the production of light olefins from ex-situ catalytic fast pyrolysis of biomass, *Fuel Process. Technol.* 210 (2020) 106562.
- [53] W. Huang, F. Gong, M. Fan, Q. Zhai, C. Hong, Q. Li, Production of light olefins by catalytic conversion of lignocellulosic biomass with HZSM-5 zeolite impregnated with 6wt.% lanthanum, *Bioresour. Technol.* 121 (2012) 248–255.
- [54] S. Zhang, M. Yang, J. Shao, H. Yang, K. Zeng, Y. Chen, J. Luo, F.A. Agblevor, H. Chen, The conversion of biomass to light olefins on Fe-modified ZSM-5 catalyst: effect of pyrolysis parameters, *Sci. Total Environ.* 628 (2018) 350–357.
- [55] M. Yang, J. Shao, H. Yang, Y. Chen, X. Bai, S. Zhang, H. Chen, Catalytic pyrolysis of hemicellulose for the production of light olefins and aromatics over Fe modified ZSM-5 catalysts, *Cellulose* 26 (2019) 8489–8500.
- [56] J. Shao, C. Jia, X. Chen, J. Luo, Y. Chen, H. Yang, H. Chen, Enhancing the production of light olefins from wheat straw with modified HZSM-5 catalytic pyrolysis, *Energy Fuel* 33 (2019) 11263–11273.
- [57] D.T. Sekyere, J. Zhang, Y. Chen, Y. Huang, M. Wang, J. Wang, N. Niwamanya, A. Barigye, Y. Tian, Production of light olefins and aromatics via catalytic co-pyrolysis of biomass and plastic, *Fuel* 333 (2023) 126339.
- [58] I. Yarulina, A.D. Chowdhury, F. Meirer, B.M. Weckhuysen, J. Gascon, Recent trends and fundamental insights in the methanol-to-hydrocarbons process, *Nat. Catal.* 1 (2018) 398–411.
- [59] S. Zhang, M. Yang, J. Shao, H. Yang, K. Zeng, Y. Chen, J. Luo, F.A. Agblevor, H. Chen, The conversion of biomass to light olefins on Fe-modified ZSM-5 catalyst: effect of pyrolysis parameters, *Sci. Total Environ.* 628–629 (2018) 350–357.
- [60] J. Shang, G. Fu, Z. Cai, X. Feng, Y. Tuo, X. Zhou, H. Yan, C. Peng, X. Jin, Y. Liu, X. Chen, C. Yang, D. Chen, Regulating light olefins or aromatics production in ex-situ catalytic pyrolysis of biomass by engineering the structure of tin modified ZSM-5 catalyst, *Bioresour. Technol.* 330 (2021) 124975.
- [61] V.P.S. Caldeira, A. Peral, M. Linares, A.S. Araujo, R.A. Garcia-Muñoz, D. P. Serrano, Properties of hierarchical beta zeolites prepared from protozeolitic nanonits for the catalytic cracking of high density polyethylene, *Appl. Catal. A Gen.* 531 (2017) 187–196.
- [62] E. Selvam, P.A. Kots, B. Hernandez, A. Malhotra, W. Chen, J.M. Catala-Civera, J. Santamaria, M. Ierapetritou, D.G. Vlachos, Plastic waste upgrade to olefins via mild slurry microwave pyrolysis over solid acids, *Chem. Eng. J.* 454 (2023) 140332.
- [63] T. Nandakumar, U. Dwivedi, K.K. Pant, S. Kumar, E. Balaraman, Wheat straw/HDPE co-reaction synergy and enriched production of aromatics and light olefins via catalytic co-pyrolysis over Mn, Ni, and Zn metal modified HZSM-5, *Catal. Today* 408 (2023) 111–126.
- [64] H. Zhang, Y.-T. Cheng, T.P. Vispute, R. Xiao, G.W. Huber, Catalytic conversion of biomass-derived feedstocks into olefins and aromatics with ZSM-5: the hydrogen to carbon effective ratio, *Energy Environ. Sci.* 4 (2011) 2297–2307.
- [65] E.T. Vogt, B.M. Weckhuysen, Fluid catalytic cracking: recent developments on the grand old lady of zeolite catalysis, *Chem. Soc. Rev.* 44 (2015) 7342–7370.
- [66] A. Corma, J. Mengual, P.J. Miguel, IM-5 zeolite for steam catalytic cracking of naphtha to produce propene and ethene. An alternative to ZSM-5 zeolite, *Appl. Catal. A Gen.* 460 (2013) 106–115.
- [67] A.G. Gayubo, B. Valle, A.T. Aguayo, M. Olazar, J. Bilbao, Olefin production by catalytic transformation of crude bio-oil in a two-step process, *Ind. Eng. Chem. Res.* 49 (2010) 123–131.
- [68] T.P. Vispute, H. Zhang, A. Sanna, R. Xiao, G.W. Huber, Renewable chemical commodity feedstocks from integrated catalytic processing of pyrolysis oils, *Science* 330 (2010) 1222–1227.
- [69] F. Gong, Z. Yang, C. Hong, W. Huang, S. Ning, Z. Zhang, Y. Xu, Q. Li, Selective conversion of bio-oil to light olefins: controlling catalytic cracking for maximum olefins, *Bioresour. Technol.* 102 (2011) 9247–9254.
- [70] C. Hong, F. Gong, M. Fan, Q. Zhai, W. Huang, T. Wang, Q. Li, Selective production of green light olefins by catalytic conversion of bio-oil with Mg/HZSM-5 catalyst, *J. Chem. Technol. Biotechnol.* 88 (2013) 109–118.
- [71] W. Huang, F. Gong, M. Fan, Q. Zhai, C. Hong, Q. Li, Production of light olefins by catalytic conversion of lignocellulosic biomass with HZSM-5 zeolite impregnated with 6 wt.% lanthanum, *Bioresour. Technol.* 121 (2012) 248–255.
- [72] M. Kusenberger, G.C. Fausson, H.D. Thi, M. Roosen, M. Grlic, A. Eschenbacher, S. De Meester, K.M. Van Geem, Maximizing olefin production via steam cracking of distilled pyrolysis oils from difficult-to-recycle municipal plastic waste and marine litter, *Sci. Total Environ.* 838 (2022) 156092.
- [73] M. Materazzi, M. Materazzi, Gasification of Waste Derived Fuels in Fluidized Beds: Fundamental Aspects and Industrial Challenges, clean Energy from Waste: Fundamental Investigations on Ashes and Tar Behaviours in a Two Stage Fluid Bed-Plasma Process for Waste Gasification, 2017, pp. 19–63.
- [74] S. Cao, J. Cao, H. Zhu, Y. Huang, B. Jin, M. Materazzi, Removal of HCl from gases using modified calcined Mg-Al-CO₃ hydrotalcite: performance, mechanism, and adsorption kinetics, *Fuel* 355 (2024) 129445.
- [75] M. Shahabuddin, M.T. Alam, B.B. Krishna, T. Bhaskar, G. Perkins, A review on the production of renewable aviation fuels from the gasification of biomass and residual wastes, *Bioresour. Technol.* 312 (2020) 123596.
- [76] H. Zhu, Z. Chen, L. Pastor-Perez, X. Long, M. Millan, How syngas composition affects catalytic steam reforming of tars: an analysis using toluene as model compound, *Int. J. Hydrog. Energy* 48 (2023) 1290–1303.
- [77] J. Kopycinski, T.J. Schildhauer, S.M.A. Biollal, Production of synthetic natural gas (SNG) from coal and dry biomass – A technology review from 1950 to 2009, *Fuel*, 89 (2010) 1763–1783.
- [78] V.N. Raibhole, S.N. Sapali, Simulation and parametric analysis of cryogenic oxygen plant for biomass gasification, *Mech. Eng. Res.* 2 (2012) 97.
- [79] R.G.D. Santos, A.C. Alencar, Biomass-derived syngas production via gasification process and its catalytic conversion into fuels by Fischer Tropsch synthesis: a review, *Int. J. Hydrog. Energy* 45 (2020) 18114–18132.
- [80] Y. Xu, X. Li, J. Gao, J. Wang, G. Ma, X. Wen, Y. Yang, Y. Li, M. Ding, A hydrophobic FeMn@Si catalyst increases olefins from syngas by suppressing C1 by-products, *Science* 371 (2021) 610–613.
- [81] H.L. Zhu, L. Pastor-Pérez, M. Millan, Catalytic steam reforming of toluene: understanding the influence of the main reaction parameters over a reference catalyst, *Energies* 13 (2020) 813.
- [82] A. Nanduri, S.S. Kulkarni, P.L. Mills, Experimental techniques to gain mechanistic insight into fast pyrolysis of lignocellulosic biomass: a state-of-the-art review, *Renew. Sust. Energy Rev.* 148 (2021) 111262.
- [83] M. Dry, The Fischer-tropsch synthesis, *Catal. Sci. Technol.* 1 (1981) 159–255.
- [84] R.N. Kumar, V. Aarthi, From biomass to syngas, fuels and chemicals—a review, in: AIP Conference Proceedings, AIP Publishing, 2020.
- [85] A. Yahyazadeh, A.K. Dalai, W. Ma, L. Zhang, Fischer-Tropsch synthesis for light olefins from syngas: a review of catalyst development, *Reactions* 2 (2021) 227–257.
- [86] W.M. Sachtler, The second Rideal lecture. What makes a catalyst selective? *Faraday Discuss. Chem. Soc.* 72 (1981) 7–31.
- [87] T.R. Keshav, S. Basu, Gas-to-liquid technologies: India's perspective, *Fuel Process. Technol.* 88 (2007) 493–500.
- [88] J. Xu, Y. Yang, Y.-W. Li, Recent development in converting coal to clean fuels in China, *Fuel* 152 (2015) 122–130.
- [89] Y. Yang, J. Xu, Z. Liu, Q. Guo, M. Ye, G. Wang, J. Gao, J. Wang, Z. Shu, W. Ge, Progress in coal chemical technologies of China, *Rev. Chem. Eng.* 36 (2019) 21–66.
- [90] Y. Liu, M. Xu, Z. Yang, X. Ding, M. Zhu, Y.-F. Han, Syngas to Olefins with low CO₂ formation by tuning the structure of FeCx-MgO-Al₂O₃ catalysts, *Chem. Eng. J.* 137167 (2022).
- [91] Q. Chang, C. Zhang, C. Liu, Y. Wei, A.V. Cheruvathur, A.I. Dugulan, J. Niemantsverdriet, X. Liu, Y. He, M. Qing, Relationship between iron carbide phases (ε-Fe₂C, Fe₇C₃, and γ-Fe₅C₂) and catalytic performances of Fe/SiO₂ Fischer-Tropsch catalysts, *ACS Catal.* 8 (2018) 3304–3316.
- [92] K. Cheng, M. Virginie, V.V. Ordonsky, C. Cordier, P.A. Chernavskii, M. I. Ivantsov, S. Paul, Y. Wang, A.Y. Khodakov, Pore size effects in high-temperature Fischer-Tropsch synthesis over supported iron catalysts, *J. Catal.* 328 (2015) 139–150.
- [93] F. Jiang, M. Zhang, B. Liu, Y. Xu, X. Liu, Insights into the influence of support and potassium or sulfur promoter on iron-based Fischer-Tropsch synthesis: understanding the control of catalytic activity, selectivity to lower olefins, and catalyst deactivation, *Cat. Sci. Technol.* 7 (2017) 1245–1265.
- [94] X.-W. Liu, Z. Cao, S. Zhao, R. Gao, Y. Meng, J.-X. Zhu, C. Rogers, C.-F. Huo, Y. Yang, Y.-W. Li, X.-D. Wen, Iron carbides in Fischer-Tropsch synthesis: theoretical and experimental understanding in epsilon-iron carbide phase assignment, *J. Phys. Chem. C* 121 (2017) 21390–21396.
- [95] A.H. Sahir, Y. Zhang, E.C. Tan, L. Tao, Understanding the role of Fischer-Tropsch reaction kinetics in techno-economic analysis for co-conversion of natural gas and biomass to liquid transportation fuels, *Biofuels Bioprod. Biorefin.* 13 (2019) 1306–1320.
- [96] M. Ding, Y. Yang, B. Wu, Y. Li, T. Wang, L. Ma, Study on reduction and carburization behaviors of iron phases for iron-based Fischer-Tropsch synthesis catalyst, *Appl. Energy* 160 (2015) 982–989.
- [97] Z. Li, T. Lin, F. Yu, Y. An, Y. Dai, S. Li, L. Zhong, H. Wang, P. Gao, Y. Sun, M. He, Mechanism of the Mn promoter via CoMn spinel for morphology control: formation of Co₂C nanoprisms for Fischer-Tropsch to olefins reaction, *ACS Catal.* 7 (2017) 8023–8032.
- [98] N.S. Govender, F.G. Botes, M.H.J.M. de Croon, J.C. Schouten, Mechanistic pathway for C₂₊ hydrocarbons over an Fe/K catalyst, *J. Catal.* 312 (2014) 98–107.
- [99] H. Xiong, M.A. Motchelaho, M. Moyo, L.L. Jewell, N.J. Coville, Effect of Group I alkali metal promoters on Fe/CNT catalysts in Fischer-Tropsch synthesis, *Fuel* 150 (2015) 687–696.
- [100] V.V. Ordonsky, Y. Luo, B. Gu, A. Carvalho, P.A. Chernavskii, K. Cheng, A. Y. Khodakov, Soldering of iron catalysts for direct synthesis of light olefins from syngas under mild reaction conditions, *ACS Catal.* 7 (2017) 6445–6452.

- [101] J.M. Cho, C.I. Ahn, C. Pang, J.W. Bae, Fischer–Tropsch synthesis on Co/AlSBA-15: effects of hydrophilicity of supports on cobalt dispersion and product distributions, *Catalys. Sci. Technol.* 5 (2015) 3525–3535.
- [102] R.B. Anderson, W.K. Hall, A. Krieg, B. Seligman, Studies of the Fischer–Tropsch synthesis. V. Activities and surface areas of reduced and carburized cobalt catalysts, *J. Am. Chem. Soc.* 71 (1949) 183–188.
- [103] A. Yahyazadeh, B. Khoshandam, Carbon nanotube synthesis via the catalytic chemical vapor deposition of methane in the presence of iron, molybdenum, and iron–molybdenum alloy thin layer catalysts, *Results Phys.* 7 (2017) 3826–3837.
- [104] J. Lu, L. Yang, B. Xu, Q. Wu, D. Zhang, S. Yuan, Y. Zhai, X. Wang, Y. Fan, Z. Hu, Promotion effects of nitrogen doping into carbon nanotubes on supported iron Fischer–Tropsch catalysts for lower olefins, *ACS Catal.* 4 (2014) 613–621.
- [105] B. Chen, X. Zhang, W. Chen, D. Wang, N. Song, G. Qian, X. Duan, J. Yang, D. Chen, W. Yuan, X. Zhou, Tailoring of Fe/MnK-CNTs composite catalysts for the Fischer–Tropsch synthesis of lower olefins from syngas, *Ind. Eng. Chem. Res.* 57 (2018) 11554–11560.
- [106] Y. Liu, J.-F. Chen, Y. Zhang, The effect of pore size or iron particle size on the formation of light olefins in Fischer–Tropsch synthesis, *RSC Adv.* 5 (2015) 29002–29007.
- [107] Z. Ni, H. Qin, S. Kang, J. Bai, Z. Wang, Y. Li, Z. Zheng, X. Li, Effect of graphitic carbon modification on the catalytic performance of Fe@ SiO₂-GC catalysts for forming lower olefins via Fischer–Tropsch synthesis, *J. Colloid Interface Sci.* 516 (2018) 16–22.
- [108] H.M.T. Galvis, A.C. Koeken, J.H. Bitter, T. Davidian, M. Ruitenbeek, A.I. Dugulan, K.P. de Jong, Effects of sodium and sulfur on catalytic performance of supported iron catalysts for the Fischer–Tropsch synthesis of lower olefins, *J. Catal.* 303 (2013) 22–30.
- [109] M. Zhao, C. Yan, S. Jinchang, Z. Qianwen, Modified iron catalyst for direct synthesis of light olefin from syngas, *Catal. Today* 316 (2018) 142–148.
- [110] Y. Xu, X. Jia, X. Liu, Supported Fe/MnO_x catalyst with Ag doping for remarkably enhanced catalytic activity in Fischer–Tropsch synthesis, *Catalys. Sci. Technol.* 8 (2018) 1953–1970.
- [111] S. Zhang, D. Li, Y. Liu, Y. Zhang, Q. Wu, Zirconium doped precipitated Fe-based catalyst for Fischer–Tropsch synthesis to light olefins at industrially relevant conditions, *Catal. Lett.* 149 (2019) 1486–1495.
- [112] S. Mehariya, A. Iovine, P. Casella, D. Musmarra, A. Figoli, T. Marino, N. Sharma, A. Molino, Chapter 7 - Fischer–Tropsch synthesis of syngas to liquid hydrocarbons, in: A. Yousuf, D. Pirozzi, F. Sannino (Eds.) *Lignocellulosic Biomass to Liquid Biofuels*, Academic Press, 2020, pp. 217–248.
- [113] P. Tian, Y. Wei, M. Ye, Z. Liu, Methanol to olefins (MTO): from fundamentals to commercialization, *ACS Catal.* 5 (2015) 1922–1938.
- [114] M.R. Gogate, Methanol-to-olefins process technology: current status and future prospects, *Pet. Sci. Technol.* 37 (2019) 559–565.
- [115] J.A. Moulijn, M. Makkee, A.E. Van Diepen, *Chemical Process Technology*, John Wiley & Sons, 2013.
- [116] X. Wu, S. Xu, Y. Wei, W. Zhang, J. Huang, S. Xu, Y. He, S. Lin, T. Sun, Z. Liu, Evolution of C–C bond formation in the methanol-to-olefins process: from direct coupling to autocatalysis, *ACS Catal.* 8 (2018) 7356–7361.
- [117] J. Li, Z. Wei, Y. Chen, B. Jing, Y. He, M. Dong, H. Jiao, X. Li, Z. Qin, J. Wang, A route to form initial hydrocarbon pool species in methanol conversion to olefins over zeolites, *J. Catal.* 317 (2014) 277–283.
- [118] T. Sun, W. Chen, S. Xu, A. Zheng, X. Wu, S. Zeng, N. Wang, X. Meng, Y. Wei, Z. Liu, The first carbon-carbon bond formation mechanism in methanol-to-hydrocarbons process over chabazite zeolite, *Chem* 7 (2021) 2415–2428.
- [119] A.D. Chowdhury, K. Houben, G.T. Whiting, M. Mokhtar, A.M. Asiri, S.A. Al-Thabaiti, S.N. Basahel, M. Baldus, B.M. Weckhuysen, Initial carbon–carbon bond formation during the early stages of the methanol-to-olefin process proven by zeolite-trapped acetate and methyl acetate, *Angew. Chem.* 128 (2016) 16072–16077.
- [120] X. Liu, W. Zhou, Y. Yang, K. Cheng, J. Kang, L. Zhang, G. Zhang, X. Min, Q. Zhang, Y. Wang, Design of efficient bifunctional catalysts for direct conversion of syngas into lower olefins via methanol/dimethyl ether intermediates, *Chem. Sci.* 9 (2018) 4708–4718.
- [121] T. Mole, G. Bett, D. Seddon, Conversion of methanol to hydrocarbons over ZSM-5 zeolite: an examination of the role of aromatic hydrocarbons using ¹³C-carbon- and deuterium-labeled feeds, *J. Catal.* 84 (1983) 435–445.
- [122] M. Bjørgen, S. Svelle, F. Joensen, J. Nerlov, S. Kolboe, F. Bonino, L. Palumbo, S. Bordiga, U. Olsbye, Conversion of methanol to hydrocarbons over zeolite H-ZSM-5: on the origin of the olefinic species, *J. Catal.* 249 (2007) 195–207.
- [123] J.F. Haw, W. Song, D.M. Marcus, J.B. Nicholas, The mechanism of methanol to hydrocarbon catalysis, *Acc. Chem. Res.* 36 (2003) 317–326.
- [124] J. Zhong, J. Han, Y. Wei, Z. Liu, Catalysts and shape selective catalysis in the methanol-to-olefin (MTO) reaction, *J. Catal.* 396 (2021) 23–31.
- [125] J. Li, Y. Wei, J. Chen, S. Xu, P. Tian, X. Yang, B. Li, J. Wang, Z. Liu, Cavity controls the selectivity: insights of confinement effects on MTO reaction, *ACS Catal.* 5 (2015) 661–665.
- [126] W. Zhang, J. Chen, S. Xu, Y. Chu, Y. Wei, Y. Zhi, J. Huang, A. Zheng, X. Wu, X. Meng, Methanol to olefins reaction over cavity-type zeolite: cavity controls the critical intermediates and product selectivity, *ACS Catal.* 8 (2018) 10950–10963.
- [127] K. Cheng, B. Gu, X. Liu, J. Kang, Q. Zhang, Y. Wang, Direct and highly selective conversion of synthesis gas into lower olefins: design of a bifunctional catalyst combining methanol synthesis and carbon–carbon coupling, *Angew. Chem. Int. Ed.* 55 (2016) 4725–4728.
- [128] Y. Ni, Y. Liu, Z. Chen, M. Yang, H. Liu, Y. He, Y. Fu, W. Zhu, Z. Liu, Realizing and recognizing syngas-to-olefins reaction via a dual-bed catalyst, *ACS Catal.* 9 (2018) 1026–1032.
- [129] K. Gong, Y. Wei, Y. Dai, T. Lin, F. Yu, Y. An, X. Wang, F. Sun, Z. Jiang, L. Zhong, Carbon-encapsulated metallic Co nanoparticles for Fischer–Tropsch to olefins with low CO₂ selectivity, *Appl. Catal. B Environ.* 316 (2022) 121700.
- [130] E. de Smit, B.M. Weckhuysen, The renaissance of iron-based Fischer–Tropsch synthesis: on the multifaceted catalyst deactivation behaviour, *Chem. Soc. Rev.* 37 (2008) 2758–2781.
- [131] W. Ma, G. Jacobs, D.E. Sparks, B. Todic, D.B. Bukur, B.H. Davis, Quantitative comparison of iron and cobalt based catalysts for the Fischer–Tropsch synthesis under clean and poisoning conditions, *Catal. Today* 343 (2020) 125–136.
- [132] V.R.R. Pendyala, W.D. Shafer, G. Jacobs, M. Martinelli, D.E. Sparks, B.H. Davis, Fischer–Tropsch synthesis: effect of ammonia on product selectivities for a Pt promoted Co/alumina catalyst, *RSC Adv.* 7 (2017) 7793–7800.
- [133] W. Ma, G. Jacobs, B. Legras, S. Paul, M. Virginie, V.L. Sushkevich, A. Y. Khodakov, Effects of co-feeding with nitrogen-containing compounds on the performance of supported cobalt and iron catalysts in Fischer–Tropsch synthesis, *Catal. Today* 275 (2016) 84–93.
- [134] L. Gavrilović, J. Brandin, A. Holmen, H.J. Venvik, R. Myrstad, E.A. Blekkan, Fischer–Tropsch synthesis—Investigation of the deactivation of a Co catalyst by exposure to aerosol particles of potassium salt, *Appl. Catal. B Environ.* 230 (2018) 203–209.
- [135] R.Y. Brogaard, R. Henry, Y. Schuurman, A.J. Medford, P.G. Moses, P. Beato, S. Svelle, J.K. Nørskov, U. Olsbye, Methanol-to-hydrocarbons conversion: the alkene methylation pathway, *J. Catal.* 314 (2014) 159–169.
- [136] I.B. Minova, M. Bühl, S.K. Matam, C.R.A. Catlow, M.D. Frogley, G. Cinque, P. A. Wright, R.F. Howe, Carbene-like reactivity of methoxy groups in a single crystal SAPO-34 MTO catalyst, *Catalysis, For. Sci. Technol.* 12 (2022) 2289–2305.
- [137] Y. Ni, Y. Liu, Z. Chen, M. Yang, H. Liu, Y. He, Y. Fu, W. Zhu, Z. Liu, Realizing and recognizing Syngas-to-Olefins reaction via a dual-bed catalyst, *ACS Catal.* 9 (2019) 1026–1032.
- [138] Z. Liu, Y. Ni, M. Gao, L. Wang, X. Fang, J. Liu, Z. Chen, N. Wang, P. Tian, W. Zhu, Z. Liu, simultaneously achieving high conversion and selectivity in Syngas-to-Propane reaction via a dual-bed catalyst system, *ACS Catal.* 12 (2022) 3985–3994.
- [139] V.S. Sikarwar, M. Zhao, Biomass gasification, in: M.A. Abraham (Ed.), *Encyclopedia of Sustainable Technologies*, Elsevier, Oxford, 2017, pp. 205–216.
- [140] S. Iannello, S. Morrin, M. Materazzi, Fluidised bed reactors for the thermochemical conversion of biomass and waste, *Kona Powder Part. J.* 37 (2020) 114–131.
- [141] Y. Xu, X. Li, M. Ding, Techno-economic analysis of olefin production based on Fischer–Tropsch synthesis, *Chem* 7 (2021) 1977–1980.
- [142] F. Keller, R.P. Lee, B. Meyer, Life cycle assessment of global warming potential, resource depletion and acidification potential of fossil, renewable and secondary feedstock for olefin production in Germany, *J. Clean. Prod.* 250 (2020) 119484.
- [143] E.A.R. Zuiderveen, K.J.J. Kuipers, C. Caldeira, S.V. Hanssen, M.K. van der Hulst, M.M.J. de Jonge, A. Vlysidis, R. van Zelm, S. Sala, M.A.J. Huijbregts, The potential of emerging bio-based products to reduce environmental impacts, *Nat. Commun.* 14 (2023) 8521.
- [144] A. Reznichenko, A. Harlin, Next generation of polyolefin plastics: improving sustainability with existing and novel feedstock base, *SN Appl. Sci.* 4 (2022) 108.
- [145] M. Bachmann, S. Völker, J. Kleinekorte, A. Bardow, Syngas from what? Comparative life-cycle assessment for syngas production from biomass, CO₂, and steel mill off-gases, *ACS Sustain. Chem. Eng.* 11 (2023) 5356–5366.
- [146] S. Mahapatra, D. Kumar, B. Singh, P.K. Sachan, Biofuels and their sources of production: a review on cleaner sustainable alternative against conventional fuel, in the framework of the food and energy nexus, *Energy Nexus* 4 (2021) 100036.
- [147] J. Sherwood, The significance of biomass in a circular economy, *Bioresour. Technol.* 300 (2020) 122755.